Conference Materials

PRO-TECH-MA 2025

The Progressive Technologies and Materials in Mechanical Engineering

The International Conference

PRO TECH MA

25-27 June 2025, Sandomierz, Poland

Lublin 2025

Organisation Committee

Scientific Committee

Table of contents

Stanisław Kut[1], *Grażyna Ryzińska*[2]

The influence of the type of test in determining the constitutive equations of hyperelastic bodies

Abstract

This paper presents the results of research aimed at assessing the effectiveness of four selected constitutive equations for hyperelastic bodies in numerical modeling of the first compression load cycle. An polyurethane elastomer with a hardness of 90 ShA was used for the tests. The constitutive equations selected for the study are: 1. - Neo-Hookean, 2. - James Green Simpson, 3. - Arruda Boyce and 4. - Gent.

An analysis was carried out for four variants of determining the constants in the constitutive equations. In variants I, II and III, the material constants were determined on the basis of a single material test, i.e. the most popular and available in engineering practice, the uniaxial tensile test (variant I), the biaxial tensile test (variant II) and the tensile test in a plane strain (variant III). In variant IV, the constants in the constitutive equations were determined on the basis of all three above material tests. The accuracy of the obtained results was verified experimentally. An important stage of the research was development of stress-strain curve for the first load cycle of the sample on the basis of individual material tests (Fig.1.). Then, the material constants in the constitutive equations were calculated. The knowledge of the coordinates of individual points of the experimentally determined stress-strain curve is the basis for determining the values of the coefficients (material constants) in individual constitutive equations. In this work MSC Marc / Mentat 2020 was used to determine the constants in the constitutive equations selected for the study. After entering the coordinates of the points of the stress-strain curve determined by the experimental tests, the software adjusts the regression curves of selected constitutive models with the experimentally determined curves.

[1] The Faculty of Mechanical Engineering and Aeronautics, Rzeszow University of Technology, 12 Powstańców Warszawy Ave, Rzeszów, Poland, stan_kut@prz.edu.pl
2 The Faculty of Mechanical Engineering and Aeronautics, Rzeszow University of Technology, 12 Powstańców Warszawy Ave, Rzeszów, Poland, grar@prz.edu.pl

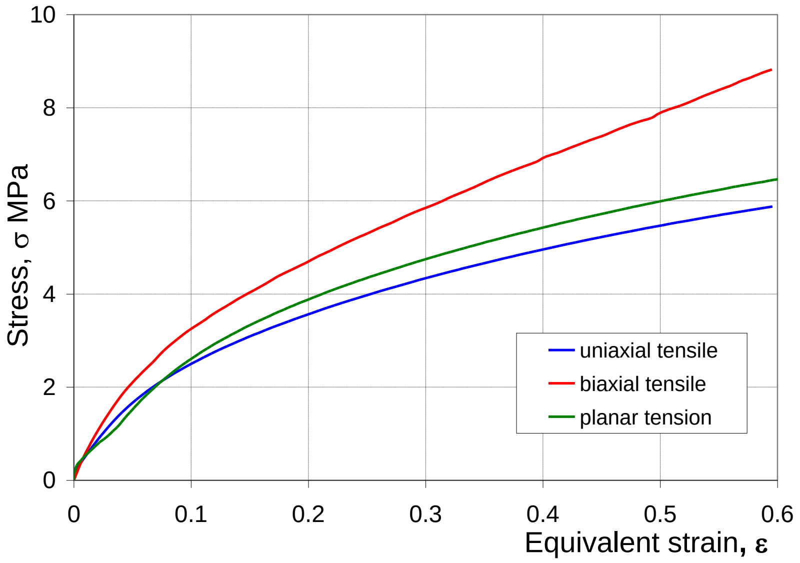

Fig.1 . Experimental stress-strain curve for the three load patterns

This adjustment can be made on the basis of data from one or more tests. Based on the fit of the curves from the individual tests, the software calculates the numerical values of the material constants for the individual constitutive equations. In this paper, the differential evolution algorithm was used to determine coefficients in the constitutive equations.

In case of modeling the behavior of an elastomer under a compressive load, the material constants in constitutive equations can be determined on the basis of the biaxial tensile test (variant II) the best. Then the modeling results do not depend on the choice of the constitutive equation or depend to a small extent. For this variant of determining the material constants, the obtained results of modeling coincide with the experiment. In the case of the models 1 -4, a similar convergence with experiment was obtained ($\psi \approx$ -9%). In the most complex variant IV, in which the constants were determined on the basis of three tests, similarly to variant II, the modeling results practically do not depend on the choice of the constitutive equation. However, despite a more complex and costly procedure of determining material constants, in variant IV, worse results were obtained than in variant II.

A large convergence of the modeling results with the experiment (higher than in variant IV) can be obtained using variant III. However, as the carried out research has shown, the effectiveness of such modeling depends on the constitutive equation used.

Marta Wójcik[1], Andrzej Skrzat[1]

Numerical simulation of the KOBO extrusion process using coupled Eulerian-Lagrangian (CEL) modeling

Abstract

The development of material forming processes and their practical application caused the need of proper describing the material behaviour at very high strain rates. The experimental determination of material properties at high strain rates is complicated and restricted by the ambiguity the methods used, as well as, the complexity of the strain phenomenon. Previous numerical simulations describing the material behaviour subjected to loading at high strain rates are necessary, therefore.

In forming processes for which the material properties depend on the strain rate, the unified plasticity theory has indicated sustainability for use. The unified plasticity theory which is related to both elasticity and plasticity theories is used for modelling the behaviour of material under loading for the wide range of temperature and strain rates including its dependence on time. It does not include the plasticity condition which is characteristic for the classical plasticity theory. Additionally, the micromechanisms of plastic deformation are also considered in a unified plasticity theory. All issues above confirm the validity of use the unified plasticity theory in numerical simulations of metals forming processes.

The unified plasticity theory is mainly based on the material model developed by the Bodner and Partom (B-P model). It is an elastic-viscoplastic model described by physical and phenomenological factors based on the continuum mechanics in order to take into account the dislocation dynamics in isothermal loading conditions, kinematic and isotropic hardening, the material damage, the relaxation and the creep, as well as the change of a temperature. More detailed information about the B-P model is described in [1-2]. The material behaviour under loading using B-P model is described using 14 temperature dependent and independent parameters contained in Table 1.

The explicit integration algorithm for the 3-D B-P model was used in this work. The method is conditionally stable but the stable time increment is very small. The input data are the total strain increment for which increments of inelastic strains and stress are determined.

[1] Department of Materials Forming and Processing, Rzeszow University of Technology, al. Powstańców Warszawy 8, 35-959, Rzeszów, m.wojcik@prz.edu.pl, askrzat@prz.edu.pl

Tab.1 Interpretation of the B-P material parameters

Parameter	Unit	Description
E	MPa	Young elastic modulus
ν	-	Poisson's ratio
D_0	s^{-1}	Limiting shear-stress rate
Z_0	MPa	Initial value of the isotropic hardening variable
Z_1	MPa	Limiting (maximum) value for isotropic hardening
Z_2	MPa	Fully recovered (minimum) value for isotropic hardening
Z_3	MPa	Limiting (maximum) value for kinematic hardening
m_1	$(MPa)^{-1}$	Hardening rate coefficient for isotropic hardening
m_2	$(MPa)^{-1}$	Hardening rate coefficient for kinematic hardening
n	-	Strain rate sensitivity parameter
A_1	s^{-1}	Recovery coefficient of isotropic hardening
A_2	s^{-1}	Recovery coefficient of kinematic hardening
r_1	-	Recovery exponent of isotropic hardening
r_2	-	Recovery exponent of kinematic hardening

The numerical simulations of the KOBO process were done using the finite element program ABAQUS. The B-P model is not included in it and therefore, its usage in the commercial software requires to write an own VUMAT procedure. The constitutive equations of the B-P model were included in a VUMAT which was written in a FORTRAN language and then was implemented into ABAQUS. The elastic-viscoplastic material with isotropic and kinematic hardening was applied. The selected results - the Huber-Mises-Henky (HMH) equivalent stress and the equivalent plastic strain (PEEQ) distributions are shown in Figure 1.

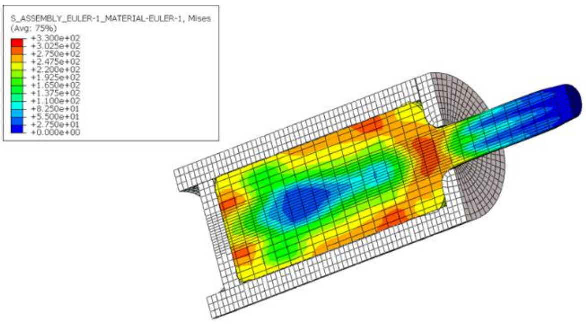
a)

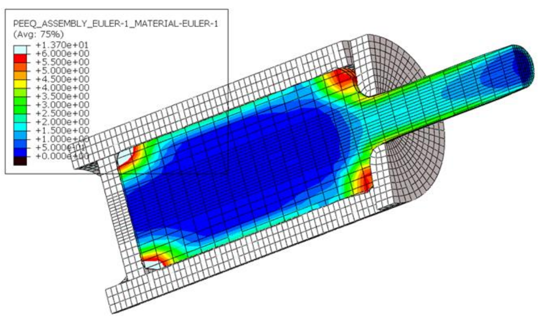
b)

Fig.1 The HMH stress (a) and the equivalent plastic strain PEEQ (b) distributions in the extruded material

References

[1] Ryzińska G., Skrzat A., Designing an impact energy-absorbing device: numerical simulations, RUTMech, 2015, 87, 349-357.

[2] Skrzat A., Application of Coupled Eulerian-Lagrangian Approach in Metal Forming Simulations, RUTMech, 2011, 84, 25-35.

Konrad Laber[1], Jacek Madura[2], Dariusz Leśniak[2], Maciej Balcerzak[2], Marek Bogusz[2]

Elaboration and verification of dedicated material models of the EN AW-7021 aluminium alloy for numerical modelling of the industrial extrusion process of profiles from difficult-to-deform aluminum alloys through portholes dies

Abstract

In order to properly design or modify existing technological processes, it is necessary to know the characteristics describing the rheological properties of the investigated material [1, 2]. For each technological process, it is possible to set of features describing the material's susceptibility to a given process can be determined. In the case of plastic working processes, the fundamental feature defining the ability of a given material to plastic forming is the yield stress and the maximum strain value [2]. In this paper, dedicated material models were elaborated and verified for three melts of the EN AW-7021 aluminium alloy with different content of zinc and magnesium [3, 4], for the extrusion process conditions of pipes with 50 mm in diameter and 2 mm of wall thickness. Based on the conducted plastometric tests, it was found that, within the tested range of strain parameters, the three analyzed melts of the same aluminium alloy were characterized by high sensitivity to both the strain rate and temperature, depending on the content of the main alloying elements. Moreover, a significant effect of magnesium and zinc content on the plasticity of the tested material was observed. Therefore, dedicated material models (mathematical models) were developed, describing changes in the yield stress as a function of strain, strain rate and temperature, for each analyzed melt.

Plastometric tests of the EN AW-7021 aluminium alloy, on the basis of which its rheological properties were determined and the yield stress function coefficients were determined, were carried out in uniaxial compression tests using the GLEEBLE 3800 metallurgical process simulator [5]. These tests were carried out in the temperature range of 450–570°C and the strain rate in the range of 0.05–5.0 s^{-1}. In order to practically use the results of plastometric tests and to obtain a mathematical relationship that makes the value of the yield

1 Faculty of Production Engineering and Materials Technology, Department of Metallurgy and Metal Technology, Czestochowa University of Technology, 19 Armii Krajowej Ave., 42-200 Czestochowa, Poland, konrad.laber@pcz.pl
2 Faculty of Non-Ferrous Metals, Department of Materials Science and Non-Ferrous Metals Engineering, AGH University of Science and Technology, Adama Mickiewicza 30 Ave., 30-059 Krakow, Poland, a) madura@agh.edu.pl, b) dlesniak@agh.edu.pl, c) balcerzak@agh.edu.pl, d) bogusz@agh.edu.pl

stress dependent on the strain parameters, the results of the tests were approximated by the Henzel-Spittel equation [6]. The developed mathematical models of the rheological properties of each melt were then implemented into the material database of the QForm-Extrusion computer software [7], which was used for the theoretical analysis of the industrial extrusion process.

In order to verify the results of numerical calculations, industrial tests of the extrusion process were carried out on a 25 MN hydraulic press with a 7-inch diameter container equipped with a process data acquisition system. The main parameters analyzed were the force parameters and the speed of the extrusion process.

Based on the obtained results, it was found that the use of three different (dedicated) material models for each melt of the analyzed aluminum alloy had a positive effect on the accuracy of the numerical modelling of the analyzed process. A high agreement was obtained regarding, among others, the theoretical and experimental extrusion force (fig. 1) and the flow rate of metal from the die hole (bearing).

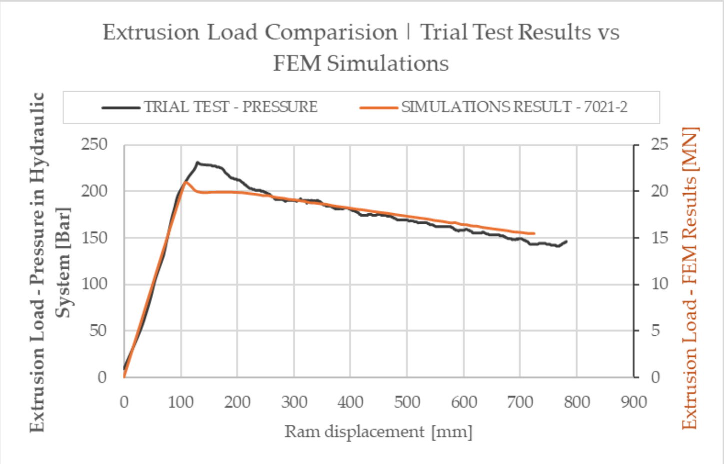

Fig. 1. Comparative graph of the force parameters of the extrusion process as a function of the punch path recorded during the trial tests (black), in relation to the values determined in the numerical simulations (orange).

References

[1]. Danchenko V.; Dyja H.; Lesik L.; Mashkin L.; Milenin A. Technologia i modelowanie procesów walcowania w wykrojach (Technology and modelling of rolling processes in grooves). Wydawnictwo Wydziału Inżynierii Procesowej, Materiałowej i Fizyki Stosowanej Politechniki Częstochowskiej (Czestochowa University of Technology, Faculty of Process, Materials Engineering and Applied Physics Publishing House), Czestochowa, Poland, 2002.

[2]. *Grosman F.; Hadasik E. Technologiczna plastyczność metali. Badania plastometryczne (Technological plasticity of metals. Plastometric tests). Wydawnictwo Politechniki Śląskiej (Silesian University of Technology Publishing House), Gliwice, Poland, 2005.*
[3]. *EN 573-1:2004 - Aluminium and aluminium alloys - Chemical composition and form of wrought products - Part 1: Numerical designation system. European Committee For Standardization 2004.*
[4]. *Leśniak D., Libura W., Leszczyńska-Madej B., Bogusz M., Madura J., Płonka B., Boczkal S., Jurczak H. FEM Numerical and Experimental Work on Extrusion Welding of 7021 Aluminum Alloy. Materials 2023, Volume 16, Issue 17, https:// doi.org/10.3390/ma16175817.*
[5]. *Praca zbiorowa pod redakcją (Collective work edited by) J. Siwka i J. Wysłocki. Rozwój badań naukowych w dziedzinie nauk technicznych i fizycznych (Development of scientific research in the field of technical and physical sciences). Wydawnictwo Wydziału Inżynierii Procesowej, Materiałowej i Fizyki Stosowanej Politechniki Częstochowskiej (Publishing House of the Faculty of Process Engineering, Materials Engineering and Applied Physics of the Czestochowa University of Technology), Czestochowa, Poland, 2005.*
[6]. *Henzel A., Spittel T.: Rasciet energosilovykh parametrov v processakh obrobotki metallov davlenijem, Metalurgija, Moskva 1982.*
[7]. *Biba N., Stebunov S., Vlasov A. Application of QForm Program for Improvement of the Die Design and Profile Extrusion Technology. In Proceedings of the Ninth International Aluminum Extrusion Technology Seminar & Exposition, Orlando, USA, 2008.*

Ján Slota[1], Andrzej Kubit[1], Ivan Gajdos[1], Pavol Stefcak[1], Viliam Kapral[1]

Friction Stir Welding of Aluminum Alloys Using a Carbide Tool: Experimental and Simulation-Based Analysis

Abstract

The paper presents results of a study on the joining of sheet materials with a carbide tool. The effect of technological parameters on the quality of the joint during friction stir welding (FSW) of aluminum alloy was studied. The proper settings of welding parameters were also evaluated. Macroscopic and microscopic defects in the joints were detected using naked–eye microscopy and scanning electron microscopy (SEM). The quality of the joints was evaluated by a shear tensile test and Vickers microhardness. During the process, the axial force acting on the tool was measured as a response to varying welding conditions. It has been demonstrated that it is possible to achieve a high-quality friction stir weld joint using a WC tool. The joint strength is comparable to that of the parent material.

The FSW process was predicted by numerical simulation in the Simufact Forming software. The aim was to analyze the effects of input parameters on the simulation results and to achieve a high-quality joint with the required mechanical properties by gradual optimization. FE simulations of the FSW process were performed in both 2D and 3D settings. However, comparison of the simulation results showed that there are significant differences in the results. To achieve correct results as in 2D, it is necessary to use a very fine Tetmesh mesh in 3D. The problem, however, is that the simulation itself will take a very long time and due to self-contact, the simulation can be very unstable. A possible solution to this problem is shown in the paper.

[1] Department of Technology, Materials and Computer Supported production, Technical University of Košice, Mäsiarska 74, 040 01 Košice, Slovakia, pavol.stefcak@tuke.sk; ivan.gajdos@tuke.sk; jan.slota@tuke.sk; viliam.kapral@tuke.sk; akubit@prz.edu.pl

Tomáš Jezný[1], Gerhard Mitaľ[2],Emil Spišák[3]

Research into the tribological properties of polycarbonate produced by 3D printing using FDM technology

Abstract

This paper deals with the investigation of tribological properties of polycarbonate (PC) produced by 3D printing using Fused Deposition Modeling (FDM) technology. Samples were fabricated with different layer deposition strategies. The fabricated structures were then tested against abrasive wear. The aim of the experiment was to compare the effect of different layer deposition strategies in the 3D printing process on the abrasive wear of the material at specified process parameters. The testing conditions of the samples were followed in accordance with ASTM G65/16. Based on these tests, different strategies were compared and evaluated for their ability to resist abrasive wear.

Material and method The samples were printed with two types of placement on the printer platform. For samples 1-4, the fill strategy is applied parallel to the wear tested surface and in the second case for samples 5-9, the fill is applied perpendicular to the worn material surface. 9 strategies were printed and three samples from each strategy were labeled as M•, M••, M•••fig.1. The samples were then subjected to abrasive wear according to the ASTM G65-01 test standard.

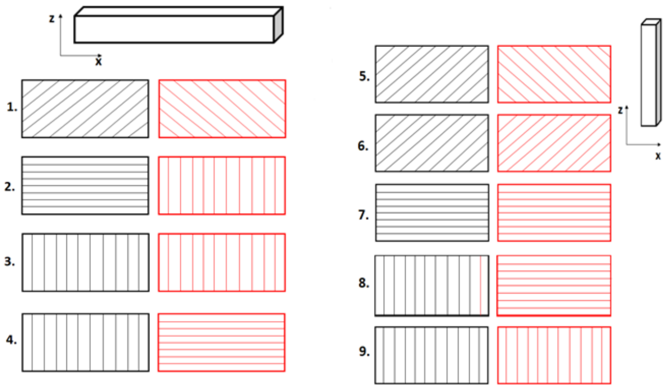

Fig.1 Applied strategies for PC samples

[1] Faculty of Mechanical Engineering, Technical University of Kosice, Mäsiarska 74, Kosice, Slovakia, tomas.jezny@tuke.sk
[2] Faculty of Mechanical Engineering, Technical University of Kosice, Mäsiarska 74, Kosice, Slovakia, gerhard.mital@tuke.sk
[3] Faculty of Mechanical Engineering, Technical University of Kosice, Mäsiarska 74, Kosice, Slovakia, emil.spisak@tuke.sk

Evaluation of the experiment From the results of the weight loss percentage experiment, it is clear that the 3D printing strategy affects the abrasive wear of individual surfaces. From the graph, we can see the lowest wear for strategies no. 1 and no. 4 (samples no. 6 and no. 7) fig.2, fig3.

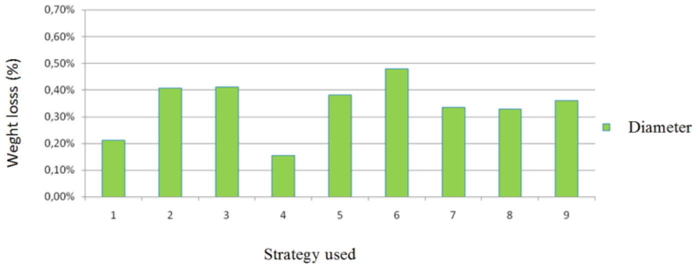

Fig.2 Average percentage of weight loss

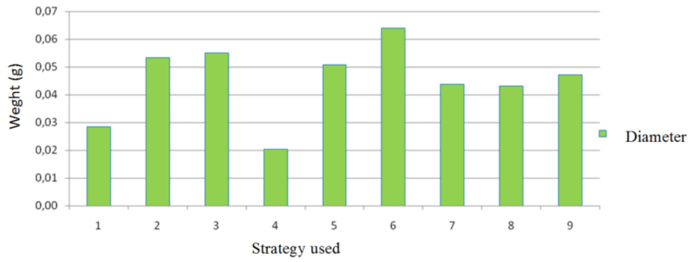

Fig.2 Weight

Conculusion

From the printing technology where the sample was with the longest edge dimension parallel to the X axis, we concluded that the most advantageous strategy for polycarbonate is No. 1. This strategy was similar to strategy No. 4 where the results were almost at the same level and therefore we can define them as strategies with the same properties against wear.

Acknowledgement

KEGA 050TUKE-4/2023 Inovácia študijných programov orientovaných na počítačovú podporu strojárskej výroby v 1. a 2. stupni vysokoškolského štúdia

References (Font 12 Times New Roman, italics)

[1] Carneiro, O.S., Silva, A.F., Gomes, R. Fused deposition modeling with polypropylene. Materials & Design, 2015, Vol. 83.

[2] Budinski, K.G., Budinski, S.T. On replacing three-body abrasion testing with three-body abrasion testing. Wear, 2017, Vol. 376-377, pp. 1859-1865. doi.org/10.1016/j.wear.2017.01.001

[3] Dodziuk, H. Applications of 3D printing in healthcare. Polish J Thoracic Cardiovas Surg, 2016, Vol. 13, No. 3, pp. 283-293.

Emil Spišák, Ema Nováková-Marcinčínová, Janka Majerníková.[1]

The Influence of Selected Technological Parameters on Additively Manufactured Metal Components Printed by Direct Laser Sintering

Abstract

The topic of the influence of selected technological parameters on additively manufactured metal components produced by Direct Laser Sintering (DLS) focuses on the study of factors that affect the quality and properties of metal products made using this advanced technology. DLS, also known as selective laser sintering, is becoming increasingly popular in the industry due to its ability to produce complex geometries and reduce material waste. However, these advantages depend on the correct setting of technological parameters, such as laser power, scanning speed, temperature, and sintering depth, which can significantly influence the final mechanical and physical properties of the components. The aim of this study is to identify key technological factors that affect the quality of additively manufactured metal parts and compare their impact on the resulting microstructure, strength, hardness, and precision. Direct Laser Sintering (DLS) is an additive technology that uses a high-energy laser to selectively melt and bond fine metal powder layer by layer. This process occurs in a protective atmosphere to prevent material oxidation. The laser energy gradually melts the powder material, which, after cooling, fuses into a solid layer, creating the desired component geometry. This process is repeated for each layer until the part is completed. The results of this study may help in more precise production process adjustments, thereby contributing to the more efficient and reliable use of DLS technology in various industrial fields.

Direct Laser Sintering (DLS) Direct Laser Sintering (DLS) is an advanced additive manufacturing process that belongs to the methods of powder metallurgy and additive material processing. This technology enables the production of three-dimensional objects by direct sintering (sintering) of metal or polymer powders in a layer-by-layer method using a high-power laser beam. The quality of the resulting part, in terms of mechanical properties, dimensional accuracy, surface roughness and internal microstructure, depends to a large extent on the optimization of the technological parameters of the process. This article focuses on the

[1] Faculty of Mechanical Engineering, Technical University of Kosice, Mäsiarska 74, Kosice, Slovakia,

key process variables that fundamentally affect the quality of the print. Operating principle DLS technology is based on a digital model (e.g. a .STL file), which is divided into thin layers. Each layer is then built up by selectively irradiating the bulk powder material with a laser and locally heating it to a temperature close to the melting or sintering point. At the laser impact points, the particles fuse together, creating a solid structure. After one layer is completed, the work surface is reduced by a defined layer height (typically 20–100 μm) and the cycle is repeated until the entire object is completed.

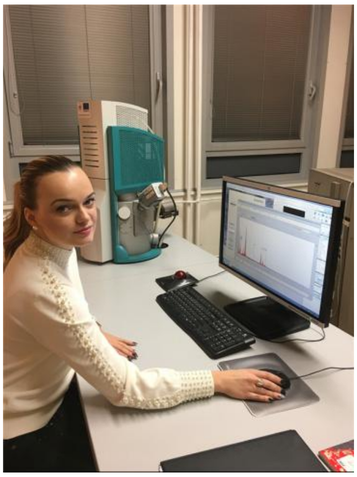

Fig.1 Microscopic testing samples from Maraging Steel MS1 material

1. Laser power and scan speed One of the most important parameters of the DLS process is the laser power (typically in the range of 100–1000 W) and its combination with the scan speed. These factors directly affect the linear energy density (LED), which is the amount of energy delivered per unit path. Too low an LED leads to insufficient sintering, porosity and poor bonding between layers, while too high an LED can cause excessive melting, deformation or evaporation of the material. The optimal power to speed ratio ensures uniform melting of the particles, thereby improving the density, strength and surface quality of the component. The laser power is usually regulated dynamically depending on the material type and object geometry.

2. Layer thickness The thickness of the individual layers (typically 20–100 μm) primarily affects the resolution and detail of the model. Thin layers allow for better rendering of fine details and achieve a smoother surface, but at the same time increase production time. Thicker layers shorten printing time, but can lead to loss of detail, higher surface roughness and weaker bonding between layers. The layer thickness must always be adapted to the properties of the powder material (especially particle size) and the requirements for the resulting part.

3. Working chamber temperature and substrate preheating The working chamber preheating is a critical parameter, especially when processing polymers and some metals, such as titanium alloys. A high and stable chamber temperature reduces the temperature gradient between layers, thereby minimizing residual stresses and the risk of deformations (e.g. twisting or cracks). Typically, the chamber is maintained just below the glass transition temperature (for polymers) or just below the melting point (for metals). Appropriate preheating also aids uniform sintering and reduces the need for post-heat treatment.

Experimental material for DLS EOS Maraging Steel MS1 – Characteristics and properties of the additive tool material EOS Maraging Steel MS1 is a high-strength iron alloy processed using Direct Metal Laser Sintering (DMLS) technology, developed by EOS GmbH. This material is intended primarily for applications that require a combination of high strength, toughness and excellent machinability, while also enabling the precise production of complex geometries. MS1 is based on the composition of maraging steel type 18Ni300 (EN 1.2709, X3NiCoMoTi18-9-5), which is known for obtaining its final mechanical properties not through carbon, but through precise precipitation hardening (aging) in the final processing phase. Uses and benefits The main advantages of EOS Maraging Steel MS1 in additive manufacturing include: • Production of complex tool components without the need for assembly, e.g. conformal cooling channels in molds. • Reduced production time compared to traditional machining and assembly of multiple parts. • Good machinability after hardening, which is advantageous for final machining of bearing surfaces or assembly elements. • Possibility of repeated heat treatment and repair of damaged areas (e.g. remelting or welding).

Conclusion

Optimization of technological parameters in Direct Laser Sintering is key to achieving high quality prints. While each parameter has its own specific impact on the result, their mutual interaction is complex and requires system adjustment with respect to the specific material, part geometry and application requirements. Modern DLS systems therefore increasingly use adaptive parameter control and advanced monitoring systems that allow real-time control of the production process. EOS Maraging Steel MS1 represents one of the most important additive metal materials in the field of toolmaking and high-strength applications. Thanks to the combination of excellent mechanical properties, precise processing and design flexibility, it offers manufacturers new possibilities in the production of functional parts and prototypes. Its successful implementation depends on correctly set printing, appropriate heat treatment and consistent quality control. The correct choice of parameters is therefore one of the main prerequisites for the successful implementation of DLS in industrial production, whether it is prototyping or serial production of functional components.

References

[1] Pustički, D.; Alar, Ž.; Bandov, Z. Additively Manufactured Maraging Steel: Influence of Heat Treatment on Corrosion and Mechanical Properties. Materials 2025, 18, 1999.

[2] Deeban, Y. Effectiveness of CAD-CAM Milled Versus DMLS Titanium Frameworks for Hybrid Denture Prosthesis: A Narrative Review. J. Funct. Biomater. 2024, 15, 376.

[3] Chen, B. Progress in Additive Manufacturing of High-Entropy Alloys. Materials 2024, 17, 5917.

[4] Bae, K.; Shin, D.; Kim, J.-H.; Lee, W.; Jo, I.; Lee, J. Influence of Post Heat Treatment Condition on Corrosion Behavior of 18Ni300 Maraging Steel Manufactured by Laser Powder Bed Fusion. Micromachines 2022, 13, 1977.

[5] Živčák, J.; Nováková-Marcinčínová, E.; Nováková-Marcinčínová, Ľ.; Balint, T.; Puškár, M. Increasing Mechanical Properties of 3D Printed Samples by Direct Metal Laser Sintering Using Heat Treatment Process. J. Mar. Sci. Eng. 2021, 9, 821.

[6] Brezinová, J.; Hudák, R.; Guzanová, A.; Draganovská, D.; Ižaríková, G.; Koncz, J. Direct Metal Laser Sintering of Ti6Al4V for Biomedical Applications: Microstructure, Corrosion Properties, and Mechanical Treatment of Implants. Metals 2016, 6, 171.

Gennady Mishuris[1]

Toughness averaging: Can we perform toughness upscaling with confidence?

Abstract

This talk will discuss whether and how an averaging-based approach to the material toughness can be confidently utilized. Usually, various upscaling procedures are applied to achieve the goal. Recently, we have proposed an averaging-based approach that is dependent not only on the material but also process dependent parameters. The respective measures come from temporal averaging (in contrast to the spacial one). They require the instantaneous crack tip velocity during each specific process. The temporal average approach is general in nature (not specific to HF), and can be used in analysis of any stable fracture propagation process.

Numerous simulations have been performed utilizing our extremely accurate and effective in-house built time-space adaptive solver, which can obtain solutions for any of the classic 1D (in space) HF models (PKN, KGD, Radial) with arbitrary fluid rheology, leak off and pumping regime. The solver uses the crack opening and the fluid velocity as the basic unknowns in contrast to the conventional crack opening and fluid pressure pair [1]. We analyse the KGD and Radial HF models in an elastic homogeneous material characterised by periodic toughness distributions (see in figure (a), one of possible instantaneous crack velocity profiles). The simulations allow us to demonstrate the temporal-averaging concept [2], showing, among others, how the effective (averaged) toughness approaches its maximum value when the crack is sufficiently long (Figure (b)).

We discuss various peculiarities of the HF propagation in such a media. In particular, we show how local energy redistribution affects the process, resulting in local (in time and space) changes of the propagation regime. For example, even if both the maximum and minimum values of the toughness distribution correspond solely to the high toughness regime (under a given fluid rate), local regions exhibiting viscosity dominated behaviour are apparent. Another interesting feature of the measures: even though the toughness and energy release rate fracture criteria are equivalent in the problem under consideration (homogeneous elastic material), temporal averaging based on the energy argument appears to be more accurate. Finally, we

[1] Department of Mathematics, Aberystwyth University, Aberystwyth, Wales, UK, ggm@aber.ac.uk

show an interesting effect of the fluid reversal within the fracture for small time fraction and questioning quasi-static approach to the HF propagating in inhomogeneous material.

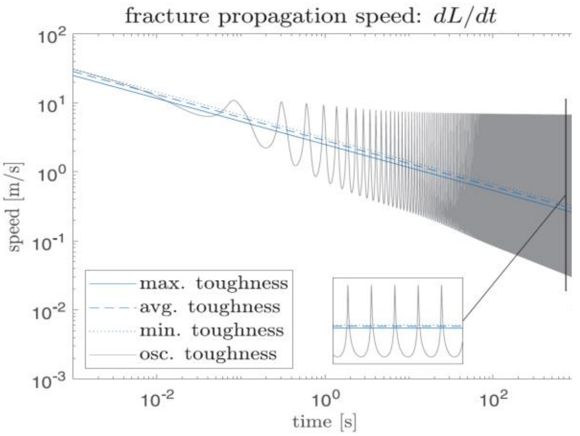

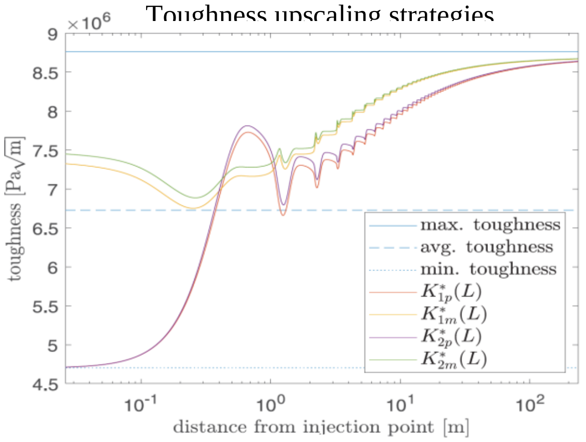

More detailed picture on the propagation of the hydraulic fracture crack in media with variable toughness can be found in [3].

Acknowledgement *The author thanks the Royal Society for Industry Fellowship.*

References

[1] Wrobel, M. Mishuris, G. (2015) Hydraulic fracture revisited: Particle velocity-based simulation. IJES, 94, 23-58, 10.1016/j.ijengsci.2015.04.003

[2] Da Fies G., Peck D., Dutko M., Mishuris G. A temporal averaging–based approach to toughness homogenisation in heterogeneous material, Mathematics and Mechanics of Solids, 2024, 29(12), 2441-2475, https://doi.org/10.1177/10812865221117553

[2] Peck D., Da Fies G., Virshilo I., Mishuris G. Peculiarities of hydraulic fracture propagation in media with heterogeneous toughness: The energy balance, elastic battery and fluid backflow, International Journal of Engineering Science, 2025, 211, 104237

Grzegorz Samołyk [1]

Simulation of casting and solidification with an example of a flowability test

Abstract

Numerical modeling is a tool commonly used in technology design [1, 2]. In the case of metal casting processes, the finite element method is most often used, although the finite difference method and the boundary element method are also used. The analysis of the casting process is typically divided into three steps: mold pouring modeling, solidification modeling, and cooling modeling. This is quite a difficult task. In the case of temperature field change calculations, the analysis is linear, while the pre-displacement of the metal in the mold is a nonlinear analysis [1].

The article concerns the use of FlowCast-3D software, which allows you to simulate the process of pouring, solidification and subsequent cooling. It allows to determine the correctness of mold cavity flooding and predict shrinkage defects. This program is based on the finite element method. The area of the mold cavity is discretized. The calculations of metal dynamics are based on the Navier-Stockes equation. Solidification analysis, on the other hand, involves identifying elements based on temperature. The advantage of this commercial program is the ability to assess the correctness of the mold filling during pouring. Unfortunately, this program allows to determine only the velocity field and the temperature field. It is not possible to perform a mechanical analysis in which the stress and strain field would be obtained. It is also impossible to analyze the cooling shrinkage, only shrinkage defects occurring during the solidification of the metal can be predicted [2, 3].

The article shows the possibility of using this commercial program to quickly estimate the quality of the product. In order to obtain a simple and unambiguous comparison of the simulation results with real conditions, the simulation refers to a basic castability test in which a spiral cavity is used. This approach also allows you to verify the material model used in the simulation, even if you abstract from the capabilities of FlowCast-3D. Examples of results are shown in Figure 1.

[1] Department of Metal Forming, Lublin University of Lublin, Poland, g.samolyk@pollub.pl

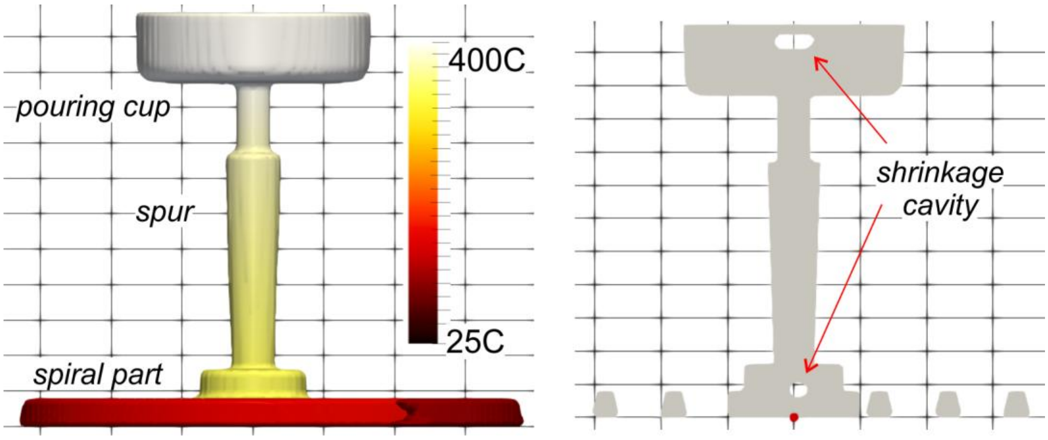

Fig.1 Temperature distribution and casting cross-section

To sum up, the proposed method is useful in quickly estimating the capabilities, not only of a commercial program, but above all of the quality of the simulation performed in this program. The castability test is a standardized and repeatable method [4]. Therefore, the comparison of the simulation results with the real sample provides a qualitative and quantitative assessment of the material model, used, for example, in databases of commercial programs.

Acknowledgement

The research was financed from the funds of the Scientific Discipline Council for Mechanical Engineering: M/KOPM/FD-20/IM-5/101

References

[1] Węgrzyn-Skrzypczak E. Numerical solution of the heat advection equation in a two-dimensional domain using the discontinuous Galerkin method. Journal of Applied Mathematics and Computational Mechanics, 2023, 22(3): 57-68

[2] Boljanovic V. Metal Shaping Proccesses: Casting and Molding. Industial Press, New York 2010.

[3] PN-H-83105:1985, Odlewy - Podział i terminologia wad.

[4] Jaśkowiec K., Uhl W., Ocena stopnia lejności staliwa aluminiowego, Prace Instytutu Odlewnictwa, Kraków 2014.

Anna Guzanová[1], Dagmar Draganovská[1], Nikita Veligotskyi[1]*

Geometric modification of mechanical joints of metallic and composite thin-walled materials in order to increase load-bearing capacity

Abstract

Thermal drilling is a technique for joining dissimilar materials by forming a sleeve, even without fasteners. For example, it is used to join thin-walled metal materials and fiber-reinforced composites [1–4]. During heating and forming the metal sleeve, the fibers in the composite are deflected, which allows the sleeve to be formed without damaging the fibers. A joint between a metal sheet and a composite formed by thermal drilling may look like the one shown in Fig. 1.

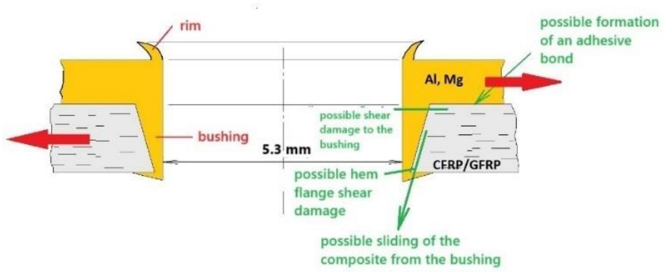

Fig.1 Schematic representation of a possible joint failure

The following materials were used for the research: The metal sheet used for the joint formation is made of EN AW 6082 T6 alloy with a thickness of 1 mm. This is a precipitation-hardened aluminum alloy, commonly used in the manufacturing of lightweight structures in the automotive industry or construction.

For the composite, polypropylene with a melting temperature of 165°C, reinforced with glass fibers (GF) and carbon fibers (CF), was used. The thickness of the composite panels was 1.5 mm, with the thickness of the glass fiber panels achieved by consolidating three layers of prepreg, while the carbon fiber panels consisted of seven layers.

The joint was created by thermal drilling using a Flowdrill Long tool ø5.3 mm, with the following process parameters: RPM 4800 min^{-1}, feed rate 60 $mm \cdot min^{-1}$. During drilling, the materials (Al-CF, Al-GF) were overlapped on a length of 30 mm.

To prevent the composite from sliding out of the bushing, a geometric modification of the bushing was proposed by forming an inverted cone with a tool of larger diameter (9.3 mm)

[1] Faculty of Mechanical Engineering, Technical University of Kosice, Mäsiarska 74, Kosice, Slovakia,

than the original bore (5.3 mm), which would eliminate the tangential component of the force that leads to the composite sliding out of the bushing, Fig. 2. The process of modifying the geometry of the bushing will be referred to as reverse drilling (RD).

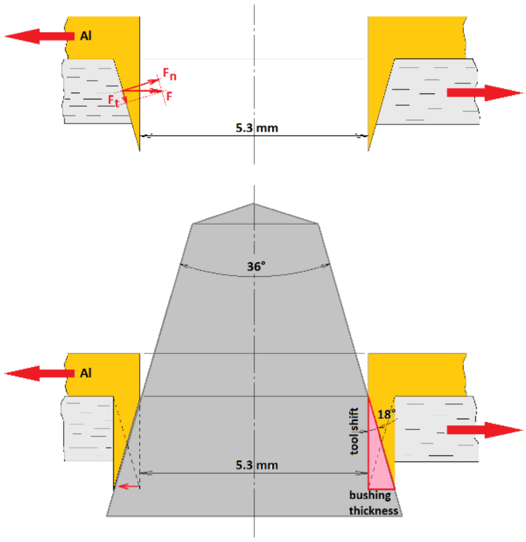

Fig.2 Design of the bushing geometry modification to increase the load carrying capacity of the connections (F - loading force, Fn - normal, Ft - tangential component of the force F)

By modifying the bushing geometry, the proportion of joints failed by bushing shear significantly increased, which was the objective of the proposed bushing modification.

Experimental tools have confirmed that by modifying the tool geometry through reverse drilling with a larger diameter tool, it is possible to achieve a more efficient utilization of the mechanical properties of metallic parts when joining metals and composites using the thermal drilling technology.

Acknowledgement *This work was supported by the Scientific Grant Agency of the Slovak Republic within the project VEGA 1/0229/23 "Research on the applicability of thermal drilling technology for the creation of multi-material joints in the automotive industry"*

References

[1] Xin Z., Liu L., Chen T., Wu L., Chen K., Kong L., Wang M., Laser surface treatment to enhance the adhesive bonding between steel and CFRP: Effect of laser spot overlapping and pulse fluence. Optics & Laser Technology, 2023, 59 , 1-12.

[2] Lambiase F.,Ko D., Two-steps clinching of aluminum and Carbon Fiber Reinforced Polymer sheets. Composite Structures, 2017, 17, 164 , 180-188.

[3] Guzanová A., Janoško E., Veligotskyi N., Optimization of joining parameters of thin-walled materials by flowdrill technology. Machines. technologies. Materials, 2022, 22, 5 , 176-178..

[4] Guzanová A., Janoško E., Application of flow-drill technology for joining metal materials. Innovations, 2021 21, 3, 108-111.

Viliam Kapraľ [1], Ivan Gajdoš [2], Dušan Manduľák [3], Volodymyr Krasinskyi [4]

Performance Evaluation of Feed Opening Section Based on Throughput Metrics

Abstract

Introduction This study presents the development, fabrication, and experimental evaluation of four 3D-printed hopper prototypes (FOS – Feed Opening Section) designed for use in polymer extrusion systems. The goal was to create functionally consistent hoppers with different shape of feed opening that could be assess the flow characteristics and throughput efficiency of various hopper geometries under controlled test conditions.

Hopper Design and 3D Printing of Functional Prototypes All hoppers were designed with a uniform hopper height of 450 mm and a wall angle of 70°. A consistent feed opening diameter of 45 mm was used across all models. To fit within the printer maximum height, the hopper height was reduced to 335 mm.

Polycarbonate (PC) filament was selected as the model material, and SR-100 was used as the support material due to geometric complexity. After printing, the inner surfaces of each hopper were smoothed to achieve uniform surface roughness, ensuring performance during material flow.

Throughput Testing of Hopper Models Comparative throughput studies were conducted using granulated pellets of sizes 2×3 mm, 3×3 mm, and 5×3 mm. For each test, 3 kg of pellets were discharged through the hopper outlet. Each pellet size was tested ten times per model.

Results Table 1 summarizes the throughput rates for each model across different pellet sizes.

[1] Department of Technology, Materials and Computer Supported Production, Technical University of Košice, Mäsiarska 74, Košice, Slovakia, viliam.kapral@tuke.sk
[2] Department of Technology, Materials and Computer Supported Production, Technical University of Košice, Mäsiarska 74, Košice, Slovakia, ivan.gajdos@tuke.sk
[3] LPH Vranov n/T, s.r.o., Pod dolami 838, Vranov n/Topľou, Slovakia, mandulak@1pn.sk
[4] Łukasiewicz Research Network – Institute of Polymer Materials, Marii Skłodowskiej-Curie 55, Toruń, Poland, volodymyr.krasinskyi@impib.lukasiewicz.gov.pl

Table 1

Pellet size, mm	Throughput of the FOS models, kg/h			
	FOS 1	FOS 2	FOS 3	FOS 4
2×3	6923 ±35	4648 ±20	3948 ±25	4473 ±25
3×3	6207 ±35	4372 ±20	3633 ±25	4120 ±25
5×3	6626 ±35	4569 ±20	3830 ±25	4450 ±25

Graph 1 shows FOS 1 consistently exhibited the highest throughput, attributed to its larger feed opening. Among the remaining hoppers, FOS 2 demonstrated superior throughput due to its geometry being most similar to FOS 1.

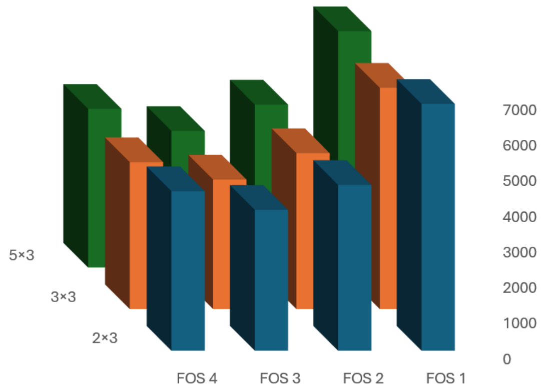

Graph 1 Throughput of the FOS models, kg/h

Conclusion

This work demonstrates the effectiveness of using 3D printing to quickly prototype and evaluate different hopper geometries for granular material flow. The methodology enabled controlled testing of discharge rates and showed how subtle geometric differences can significantly impact performance. The approach used in this study offers a practical framework for preliminary testing of bulk material handling systems using additive manufacturing technologies.

Acknowledgement: *This research was funded by the European Union's programme for research and innovation Horizon Europe under the Marie Skłodowska-Curie Action grant agreement No 101129698–PROMATAI– Horizon–MSCA–2022–SE–01. Views and opinions expressed are however those of the author(s) only and do not necessarily reflect those of the European Union or European Research Executive Agency (REA). Neither the European Union nor the granting authority can be held responsible for them.*

Peter Mulidrán[*1], *Emil Spišák*[1], *Janka Majerníková*[1], *Vladimír Rohal*[1], *Ľuboš Kaščák*[1]

Utilization of additive manufacturing for production of bending tools

Abstract

Rapid prototyping, use of FDM technology for producing forming tools is one the current research topics in the field of forming technology and design [1, 2]. Rapid prototyping offers great flexibility, reduction of costs and time in production and design of forming tools [3, 4, 5]. This article deals with the design, analysis and production of a forming die used for bending sheet metal, created using additive technology FDM (Fused Deposition Modelling) made of PLA thermoplastic. The aim was to determine to what extent it is possible to use additive manufacturing as an alternative to traditional production methods in the production of bending tools. Furthermore, a model of the bending die was designed and created in the work. Tool variants with four different percentages of infill rate (25%, 50%, 75% and 100%) were modelled and each of them was analysed using static simulations in the Solidworks Simulation software (Figure 1).

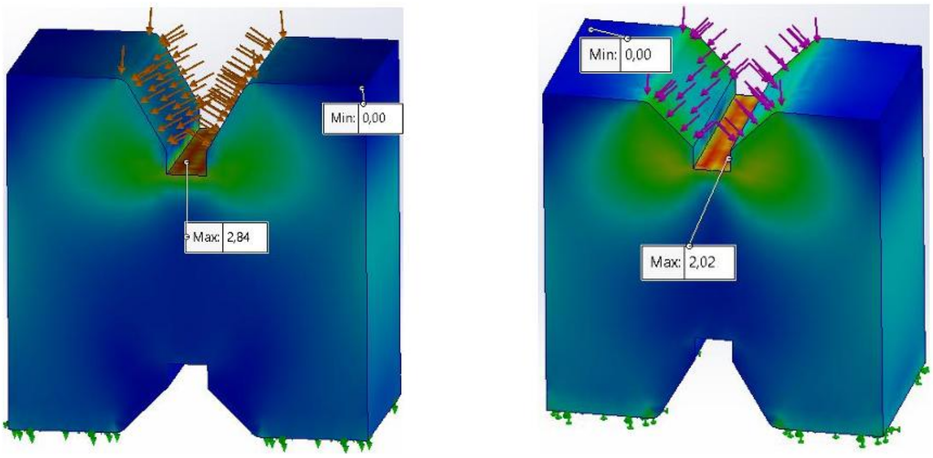

Fig.1 Stress results of static simulation of bending die made with 100 % infill rate

Tab.1 Properties of PLA tough material

Young´s modulus	Yield strength	Tensile strength	Specific weight	Poisson´s ratio
2,33 GPa	38 MPa	44 MPa	1 260 kg/m^3	0,33

*[1] Faculty of Mechanical Engineering, Technical University of Košice, Mäsiarska 74, Košice, Slovakia, peter.mulidran@tuke.sk

Tool with 100 % infill was produced and tested in V-bending process of micro-alloyed steel sheet. Bending die (Figure 2) made of PLA (Table 1) was able to withstand 6 tests of sheet metal bending with maximum force of 840 N with no visible damage or deformation.

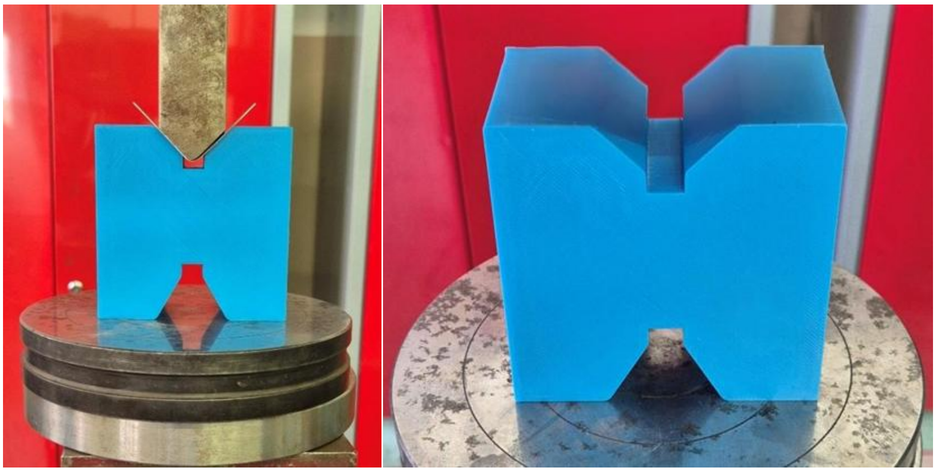

Fig.2 Bending die produced by FDM method

Acknowledgement *"The authors would like to thank Ms. Žajaková for performing numerical simulation. The authors are grateful to the VEGA 1/0330/24 for the financial support granted to cover the publication fees of this research article"*.

References

[1] L. Giorleo und E. Ceretti, "Deep drawing punches produced using fused filament fabrication technology: Performance evaluation," Journal of Manufacturing Processes, Jg. 84, S. 1–9, 2022. doi: 10.1016/j.jmapro.2022.09.054. [Online]. Verfügbar unter: https://www.sciencedirect.com/ science/article/pii/S1526612522006752

[2] G. Bergweiler, F. Fiedler, A. Shaukat und B. Löffler, "Experimental Investigation of Dimensional Precision of Deep Drawn Cups Using Direct Polymer Additive Tooling," JMMP, Jg. 5, Nr. 1, S. 3, 2021. doi: 10.3390/jmmp5010003. [Online]. Verfügbar unter: https://www.researchgate.net/publication/348001796_Experimental_Investigation_of_Dimensional_ Precision_of_Deep_Drawn_Cups_Using_Direct_Polymer_Additive_Tooling

[3] Geueke M., Steinheimer R., Lutz M. und Engel B., "Sustainable tool technology: Wood-based forming tools," Materials Research Proceedings, Jg. 28, S. 1967–1976, 2023, doi: 10.21741/9781644902479-212.

[4] M. Geueke, D. Nebeling und B. Engel, "Alternative Werkzeugtechnik – holzbasierte Umformwerkzeuge," Transformation in der Biegetechnik : Tagungsband zum 6. Biegeforum Siegen, 2023, doi: 10.25819/ubsi/10389.

[5] M. Pinto, A. D. Santos, P. Teixeira und P. J. Bolt, "Study on the usability and robustness of polymer and wood materials for tooling in sheet metal forming," Journal of Materials Processing Technology, Jg. 202, 1-3, S. 47–53, 2008, doi: 10.1016/j.jmatprotec.2007.08.082.

Jarosław Bartnicki, Janusz Tomczak[1]

Implementation of the innovative ACPF (Asymmetric Cooling Process for Forgings) technology for the production of towing hooks.

Abstract

The essence of the new solution is the implementation of asymmetric cooling technology for forgings made of 38MnVS6 and 30MnVS6 steel in order to homogenize the mechanical properties through precipitation hardening. The developed process for forgings with significant cross-sectional asymmetry was practically implemented in the conditions of the Kuźnia Matrycowa in Lublin. The heat treatment conveyor using the given solutions is 10 m long, and the time needed to complete the controlled cooling of forgings, divided into two zones, is 7-10 minutes. Cooling curves are controlled by a fan system with individual measurements and air flows in each section.

Implementation of the innovative ACPF (Asymmetric Cooling Process for Forgings) technology designed to implement the hot precipitation hardening process, guaranteeing the lowest dispersion of mechanical parameters of the finished product on the market. The solution was based on the development and implementation of a belt conveyor with separated zones guaranteeing different degrees of product cooling intensity during heat treatment. Due to the asymmetry of the manufactured products, longitudinal division was used using controlled cooling zones. The obtained results indicate the validity of using this solution, especially in terms of reducing the grain size and increasing the mechanical characteristics of the products, including the impact strength parameter, which is crucial when accepting towing hooks manufacturing process.

[1] Department of Metal Forming, Lublin University of Lublin, Poland, j.bartnicki@pollub.pl , j.tomczak@pollub.pl

Marek Kowalik[1], Rafał Kowalik[2], Paweł Maciąg[1], Piotr Paszta[3]

New tools for burnishing shafts and holes with the use of a braking torque on the burnishing roller

Abstract

Plastically deformed surface layer can be observed after all types of machining. Although it is a marginal phenomenon, it has a beneficial effect on the properties of machine parts. This is an advantageous phenomenon because the plastically deformed material has higher static and fatigue strength. The purpose of strengthening burnishing is to obtain the surface layer of the material hardened by plastic deformation. In the burnishing technology, the problem is to obtain large depths of deformation of the surface layer above 1mm. The barrier to obtaining greater depths of the deformed layer during classical roll burnishing is material cracking and pitting. The depth of the plastically deformed layer during roller burnishing can be increased to approx. 20% by applying a braking moment to the burnishing roller[1]. Burnishing with roller braking takes place in a state of asymmetric triaxial compression and the deformation of the material is more effective than when using the same pressure force in conventional roller burnishing. Studies have shown that plastic deformation in the surface layer of the material in the direction of the roller braking can be observed at a relatively small braking moment on the burnishing roller. At the Faculty of Mechanical Engineering of the Casimir Pulaski Radom University, original tools for implementing this technology on shafts and in holes were developed, which were granted patents by the Polish Patent Office.

[1] Faculty of Mechanical Engineering, Casimir Pulaski Radom University, Stasieckiego54, Radom, Poland , email:m.kowalik@uthrad.pl
[2] Institute of Technical Sciences and Aeronautics, The University College of Applied Sciences in Chełm, Pocztowa 24,Chełm, Poland
[3] Czestochowa University of Technology, Czestochowa, Poland

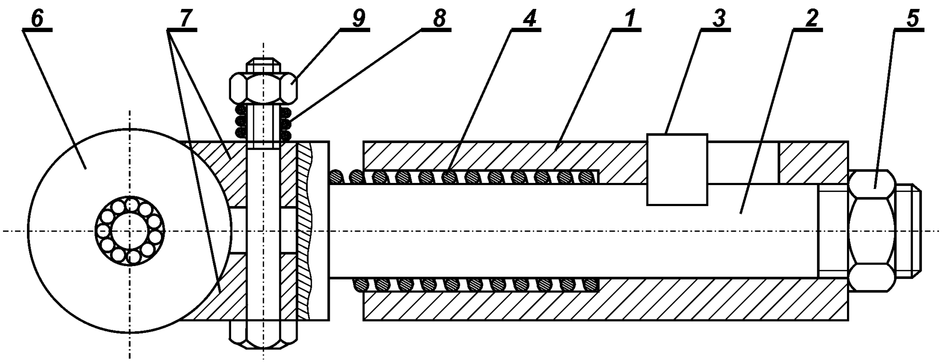

Fig.1. Burnishing device with adjustable rolling resistance force of the burnishing roller: 1-sleeve, 2-slider, 3-lip, 4-spring, 5-nut, 6-burnishing roller, 7-braking cubes, 8-roller tension spring, 9-screw and adjusting nut.[2]

At the Faculty of Mechanical Engineering of the University of Radom, original tools for implementing this technology on shafts and in holes were developed, which were granted patents by the Polish Patent Office. Fig. 1 shows a device for burnishing external surfaces of rollers Patent UPRP No. Burnishing using the device is performed as follows. The device is mounted in the lathe holder by the sleeve 1 and the roller pressure force is set, then the braking force is set by turning the nut 9, which acts on the spring 8 and the blocks 7 braking the burnishing roller 6. The spring tension force should be set so that the roller 6 does not stop during burnishing

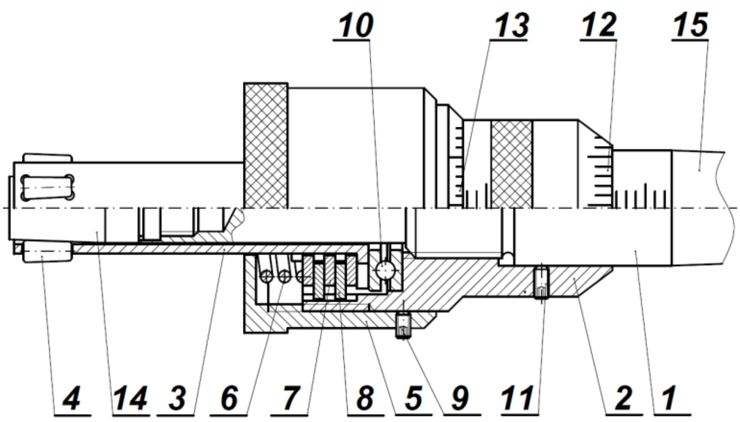

Fig. 2. Device for strengthening burnishing of holes with adjustable rolling resistance force of burnishing rollers: 1-main mandrel, 2-nut for adjusting the burnished diameter, 3-roller guide basket, 4-burnishing rollers, 5-nut for adjusting the braking torque, 6-spring of the multi-plate brake, 7-movable plate of the roller basket, 8-fixed brake plate, 9-screw for locking the set braking torque, 10-basket thrust bearing, 11-screw for locking the set burnishing diameter, 12-scale of the set diameter, 13-scale of the set braking torque, 14-replaceable track of the burnishing rollers, 15-grip part.[3]

A device for burnishing internal surfaces (holes) characterized in that the burnishing rollers are braked by a basket in which they are placed. The braking torque is set by the spring tension regulated by a locking nut. The set braking torque is transferred directly from the multi-plate brake to the burnishing roller basket.

References

[1] *Kowalik, M.; Trzepieciński, T.; Kukiełka, L.; Paszta, P.; Maciąg, P.; Legutko, S. Experimental and Numerical Analysis of the Depth of the Strengthened Layer on Shafts Resulting from Roller Burnishing with Roller Braking Moment.* Materials ***2021***, 14, *5844. https://doi.org/10.3390/ma14195844*

[2] *Kowalik, Marek. Przyrząd do nagniatania umacniającego powierzchni zewnętrznych z regulowaną siłą oporu toczenia rolki nagniatającej. Patent polski PL245623 zarejestrowany 28.05.2020 i wydany 12.06.2924.*

[3] *Kowalik, Marek, Maciąg Paweł. Przyrząd do nagniatania umacniającego otworów z regulowaną siłą oporu toczenia rolek nagniatających. Patent polski PL246764 zarejestrowany 22.12.2021 i wydany 17.07.2024*

Vladimír Rohal[1], Emil Spišák[1], Peter Mulidrán[1], Janka Majerníková[1]

Numerical Simulation of Shearing Electrical Steel

Abstract

In general, a high-quality sheared surface is characterized by low rollover height and width, a reduced fracture zone, smaller burr height and width, and a larger clean-cut zone with a 90° clean-cut angle. Numerous studies have examined the impact of clearance, the shearing gap between two blades or between the punch and die, on the quality of sheared surface. Increasing the clearance typically reduces shear quality by increasing rollover, the fracture zone, fracture angle, and burr, while decreasing the clean-cut zone. These effects are linear up to a clearance of 20–30%. Further investigation using the Cockroft & Latham failure criterion revealed that increasing the shearing gap results in a larger shear zone, leading to early material separation [1].

The shearing of electrical steel sheets under different technological conditions by help of FEM modeling was investigated by Slota et al. They found that the shear gap and the state of wear of the die and punch have a significant effect on the induced residual stress when cutting electrical steel sheets. A sharp tool edge always gives better results than a worn cutting edge. The depth of penetration of residual stresses in the region of the shear surface is significantly lower when the shearing process was performed with a smaller shear clearance. In contrast, FEM showed that smaller shear gaps can lead to higher residual stresses along the shear surface. The results show the influence of the worn cutting edge on the height of the burr [2].

For simulation purposes, the Simufact Forming 2022 simulation program was chosen. The goal of the simulation in the program was to investigate the size of the fracture surface angle β as a selected parameter of the profile of the shearing surface to predict its influence on the quality of the shearing surface when shearing experimental cut-outs.

The numerical simulation was solved in 2D, while the cutting plane passed through the very axis of the tool. For the needs of the experiment, simulations were carried out to investigate the fracture surface angle β when using different shear gaps. The measured values of the fracture surface angle β for samples from the used material, when using different shear gaps (1%, 3%,

[1] Faculty of Mechanical Engineering, Technical University of Košice, Letná 9, Košice, Slovakia, e-mail: vladimir.rohal@tuke.sk

5%, 7%, 10%), are listed in Table 1 and their graphic processing is shown in Figure 1 and Figure 2.

Tab. 1 Measured and predicted values of the fracture surface angle β in the shearing process

Sample	Thickness [MPa]	Shear gap [MPa]	Fs. Angle β – Simulation [˚]	Fs. Angle β – Experiment [˚]	Angle β difference Sim – Exp [˚]
G1	0.50	1	82,18	85,09	-2,91
G3	0.50	3	86,83	84,94	1,89
G5	0.50	5	84,41	85,94	-1,53
G7	0.50	7	83,77	80,18	3,59
G10	0.50	10	76,34	70,82	5,52

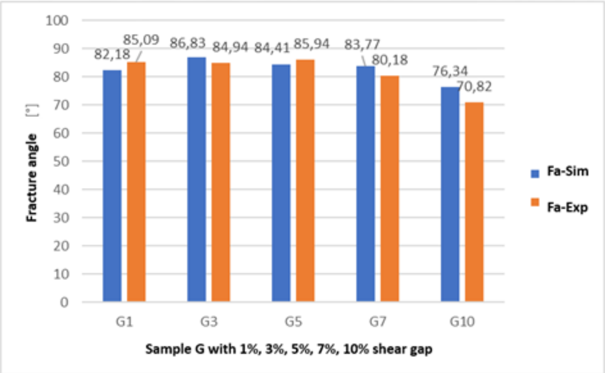

Fig. 1 Measured and predicted values of the fracture surface angle β in the shearing process

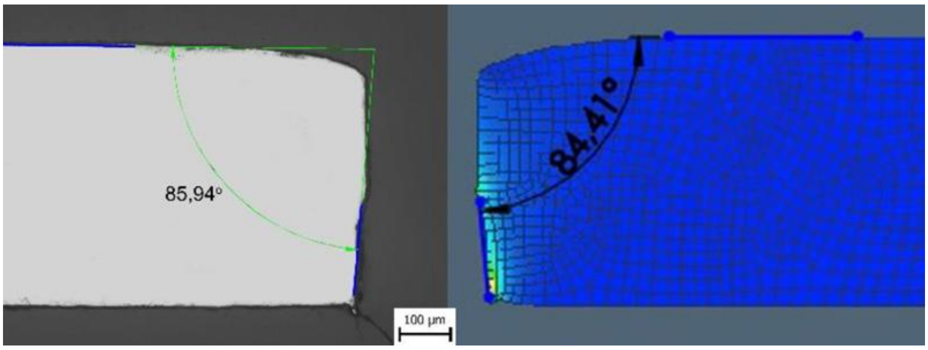

Fig. 2 Fracture surface angle β in the shearing process when using 5% shear gap

Acknowledgement *The authors are grateful to APVV-21-0418, for the financial support granted to cover the publication fees of this research article".*

References

[1] Graf, A.; Kräusel, V.; Weise, D.; Petrů, J.; Koziorek, J.; Bhandari, P. Determination of the Influence of the Tool Side Stress Superposition and Tool Geometry on the Cut Surface Quality during Precision Shear Cutting. J. Manuf. Mater. Process. 2023, 7, 145. https://doi.org/10.3390/jmmp7040145

[2] Slota J., Kaščák Ľ., Kut S.: FEM Modeling of Shear Cutting of Electrical Steel Sheets under Various Technological Conditions. In: Acta Mechanica Slovaca, č.4 (2018), s. 24-30. ISSN 1335-2393. DOI: 10.21496/ams.2018.031

Grażyna Ryzińska[1]

Influence of reinforcement type on SEA for impact energy absorbing composite elements

Abstract

In this work, experimental studies of the compression of carbon epoxy composite specimens in quasi-static conditions were performed to determine the amount of energy absorbed during this process. Specimens in the shape of pipes of two diameters were produced using a unidirectional prepreg (UD) with an areal density of 200 g/ m^2 and a plain wave prepreg (PW) with an areal density of 204 g/ m^2. Experimental studies have shown that using the UD (unidirectional) prepreg, the price of which is comparable to the PW (plain weave) prepreg, it is possible to obtain 39% greater SEA (Specific Energy Absorption) for specimens with a diameter of 20 mm and 52% more SEA for specimens with a diameter of 42 mm.

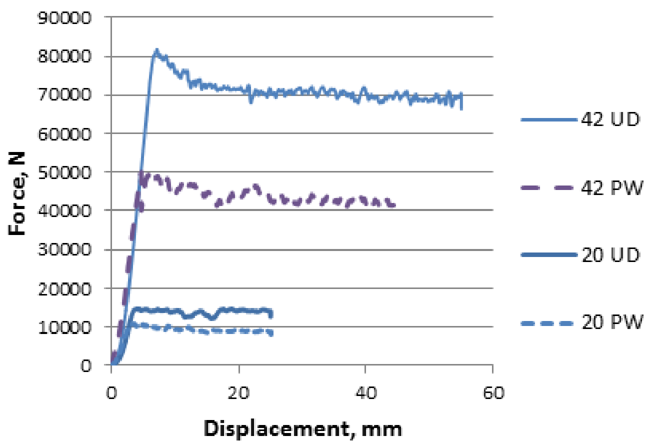

Fig. 1. Examples of force versus displacement course; 42 UD - specimen with a diameter of 42 mm UD; 42 PW - specimen with a diameter of 42 mm with a plain weave; 20 UD - specimen with a diameter of 20 mm UD; 20 PW - specimen with a diameter of 20 mm with a plain weave

The test carried out consisted of crushing the composite specimens in quasi-static conditions using a Zwick 100 kN testing machine for large specimens and a Zwick 30 kN for

1 The Faculty of Mechanical Engineering and Aeronautics, Rzeszow University of Technology, 12 Powstańców Warszawy Ave, Rzeszów, Poland, grar@prz.edu.pl

small specimens, using three specimens for each case. The testing speed in both cases was 20 mm/min. As a result of the tests, force-displacement graphs were obtained for all the cases tested (Fig.1.), determining the average force P_i and the maximum force P_{max}.

Based on all the obtained graphs, the energy was calculated, which was used to calculate the Specific Energy Absorption (SEA) according to the formula:

$$SEA = \frac{E_{tot}}{\mathrm{r}Al} \tag{1}$$

E_{tot} – total energy, ρ – average density, A – cross-sectional area, l - displacement

The obtained SEA results are summarized in the tables below (Table 1, Table 2).

Table 1. Summary of results for 20 mm diameter specimens (UD-unidirectional prepreg, PW-plain wave prepreg)

Specimen's diameter, prepreg type	Number of layers	Areal density of prepreg, g/m^2	Composite density, g/cm^3	P_i, N	P_{max}, N	SEA $_{Q-S}$, J/g	Price per 1m^2,€
20-UD	5	200	1,562	13847,31	14918,61	120,70	27
20-PW	5	204	1,453	9492,12	11096,54	86,81	29
Difference, %	0	1,96	7,50	45,88	34,44	39,03	7.41

Table 2. Summary of results for specimens with a diameter of 42 mm (UD-unidirectional prepreg, PW-plain wave prepreg)

Specimen's diameter, prepreg type	Number of layers	Areal density of prepreg, g/m^2	Composite density, g/cm^3	P_i, N	P_{max}, N	SEA $_{Q-S}$, J/g	Price per 1m^2,€
42-UD	10	200	1,562	64861,82	85279,86	132,14	27
42-PW	10	204	1,453	41135,01	52402,49	86,37	29
Difference, %	0	1,96	7,50	57,68	62,74	52,97	7.41

Using five layers of UD prepreg for specimens with a diameter of 20 mm, SEA of approx. 120 J/g can be obtained. Compared to five layers of PW prepreg, the absorbed energy SEA drops to 86 J/g. Consequently, the difference in SEA is 39% in favor of UD prepreg, additionally with a lower price of one square meter of raw material by 7%.

In the case of large specimens with a diameter of 42 mm, where ten layers of prepreg were used, the difference in the obtained SEA is almost 53% in favor of the UD prepreg, with a lower price of one square meter of this prepreg by 7%.

The maximum force Pmax obtained for specimens with a diameter of 20 mm is 14 kN for UD specimens and 11 kN for PW specimens, which gives a difference of 34% in favor of the UD prepreg. For specimens with a diameter of 42 mm, the difference is 62% in favor of the UD prepreg.

The average force Pi, which directly affects the amount of absorbed energy, is higher for specimens made of UD prepreg by 45% for smaller specimens and 57% for larger specimens, respectively.

Pavol Štefčák[1], Ivan Gajdoš[2], Ján Slota[3]

Determination of robotics additive manufacturing accuracy based on optical scanner

Abstract

Large-format additive manufacturing (LFAM) is increasingly recognized as a cost-effective and flexible approach for producing large-scale parts and components in specific industrial sectors. A key current challenge lies not only in meeting the growing demand but also in exploring new application areas and addressing emerging manufacturing constraints. Today, a range of additive manufacturing technologies are utilized in gantry-based and robotic arm-based LFAM systems. These technologies enable the fabrication of three-dimensional parts through methods such as polymer extrusion, concrete and ceramic extrusion, continuous carbon fiber extrusion combined with thermoplastic coatings, among others [1][2]. One of the main advantages of integrating industrial robots into these processes is their outstanding dexterity and flexibility, coupled with relatively low cost. However, achieving high positioning precision remains a critical aspect of robot programming that directly impacts the quality of the manufacturing outcome. Positional inaccuracies may arise from several factors, including manufacturing tolerances, parameter measurement errors, geometric deviations, and the low rigidity of robot joints [3]. Several techniques exist for measuring the position of the end-effector, each differing in terms of accuracy, complexity, the size of the calibrated workspace, cost, and data acquisition time. Commercial tools such as coordinate measuring machines (CMMs), laser interferometers, and telescoping ballbars can assess robot positioning accuracy down to a few micrometers [4]. Although prior research has evaluated the impact of workspace positioning on part accuracy, these assessments have predominantly been conducted in the context of milling applications [5].

Our paper investigates the accuracy of six-axis industrial robots in large-format additive manufacturing, focusing on the relationship between robotic repeatability and the dimensional accuracy of printed components. A total of six simple shaped samples were produced to verify the accuracy of the robot FANUC CRX-25iA equipped with pellet extruder MDPH2 (Fig. 1).

[1] Department of Technology, Materials and Computer Supported production, Technical University of Košice, Mäsiarska 74, 040 01 Košice, Slovakia, pavol.stefcak@tuke.sk
[2] ivan.gajdos@tuke.sk
[3] jan.slota@tuke.sk

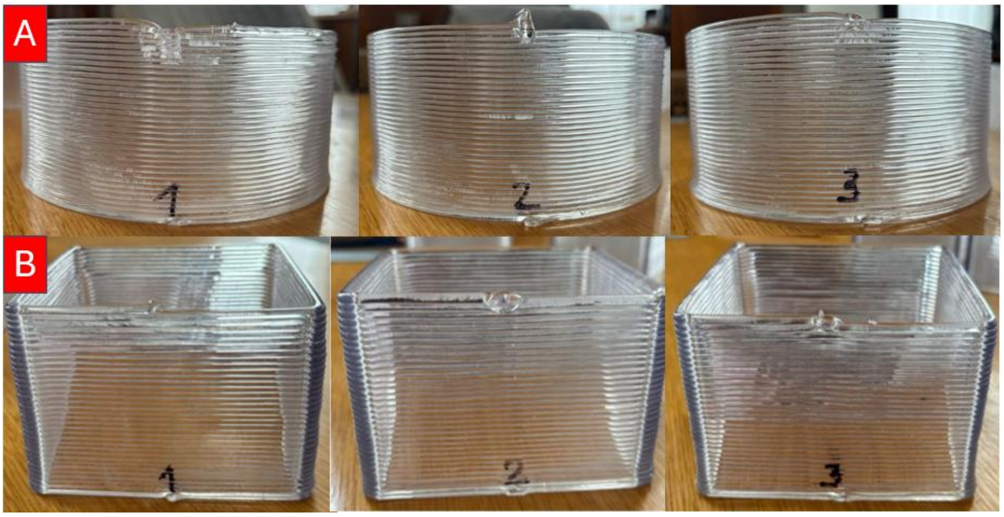

Fig.1 Samples to verify the accuracy, A- cube shape, B- Cylinder shape

The samples were then scanned (Fig. 2) on GOM scan 1 optical scanner with structured light and samples were evaluated for criteria such as material thickness, surface deviation, comparison in different cross-sections by planes ZX , ZY , flatness, parallelism and for cylindrical specimens also of circularity.

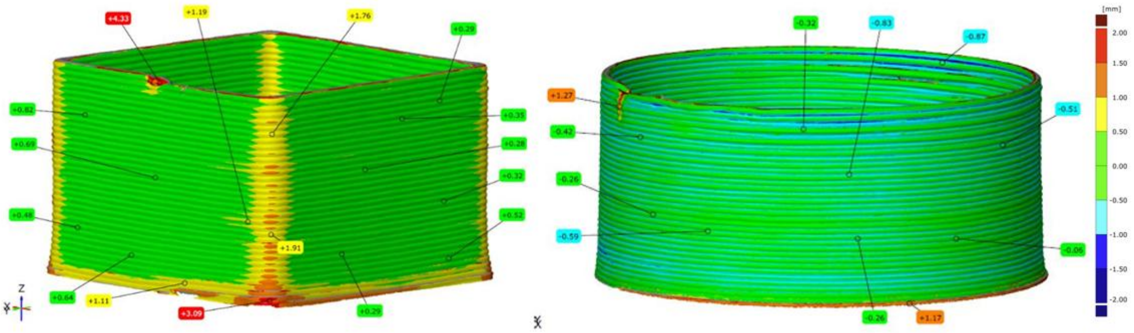

Fig.2 Evaluation of manufactured samples Cube shaped (Left) Cylinder shaped (Right)

In summary, it can be concluded that the position of the samples had an impact on the accuracy of the print and that by subsequent scanning it is possible to evaluate to what extent the accuracy of the robot was guaranteed. In the case of our workplace, the smallest deviation values were measured in the centre of the printing area, for example for the material thickness criteria of 0.61 mm for the cube and 0.76 mm for the cylinder, which then increased towards the edges of the substrate where the robot took the final position by different kinematic approaches.

Acknowledgement

This work was supported by the Slovak Research and Development Agency, project title: Research on the possibilities of forming and joining innovative metal-plastic composites in the production of lightweight thin-walled structures", project numbers: APVV SK-PL-23-0040. The authors are also grateful for the support in the experimental work to the project VEGA 1/0539/23: Research on hybrid sandwich structures with customized properties. This work was sup ported by the Slovak Research and Development Agency, project title: Research on the possibilities of forming and joining innovative metal-plastic composites in the production of lightweight thin walled structures", project numbers: SK-PL-23-0040. The authors are also grateful for the support in the experimental work to the project KEGA 050TUKE-4/2023.

The authors would also like to express their special thanks to Fanuc Slovakia company for their support in the realization of the research.

FANUC

References

[1] Paolini, A., Kollmannsberger, S., Rank, E.: Additive manufacturing in construction: a review on processes, applications, and digital planning methods. Addit. Manuf. 30, 100894 (2019)

[2] Reich, M.J., Woern, A.L., Tanikella, N.G., Pearce, J.M.: Mechanical properties and applications of recycled polycarbonate particle material extrusion-based additive manufacturing. Materials 12(10), 1642 (2019)

[3] Khanesar, M.A.; Karaca, A.; Yan, M.; Isa, M.; Piano, S.; Branson, D. Enhancing Positional Accuracy of Mechanically Modified Industrial Robots Using Laser Trackers. Robotics 2025, 14, 42. https://doi.org/10.3390/robotics14040042

[4] Slamani, Mohamed & Joubair, Ahmed & Bonev, Ilian. (2015). A comparative evaluation of three industrial robots using three reference measuring techniques. Industrial Robot: An International Journal. 42. 572-585. 10.1108/IR-05-2015-0088.

[5] Pantscharowitsch, M., Moser, L., & Kromoser, B. (2024). A study of the accuracy of industrial robots and laser-tracking for timber machining across the workspace. Wood Material Science & Engineering, 20(1), 75–93 https://doi.org/10.1080/17480272.2024.2324437

Jarosław Wójcik[1], Janusz Tomczak[1], Tomasz Kusiak[1]

The influence of tools geometry on the incremental forming process of thin-walled components

Abstract

The essence of incremental forming of thin-walled sheet metal components is the ability to manufacture products with different geometries using a single set of tools. Therefore, incremental methods have advantages over conventional methods, in which rigid tools shape a product with a geometry that reflects the shape of the tool. Among the incremental methods of shaping thin-walled components, there are known methods of single-point and multi-point incremental forming for which research is still being conducted on the influence of process parameters on the quality of shaped products [1]. Incremental forming can also be used in sheet metal bending processes, where the forming tool is a mandrel moving along a defined trajectory [2]. Spinning and flow forming methods used mainly for shaping axisymmetric components are also known [3]. When comparing conventional and incremental technologies for manufacturing sheet metal components, it is possible to note the main disadvantage of conventional methods - the need to manufacture new tools and replace them when changing the manufactured range.

Research on incremental shaping of thin-walled components is being carried out at the Lublin University of Technology. Numerical simulations of this technology were carried out and a numerical-controlled machine was designed. Fig. 1a shows the initial stage of the forming process. Attached to the machine worktable is a support on which the sheet metal is fixed. The machine worktable has the ability to move in two horizontal axes. Eventually, a rotary table will also be available. The support roller placed over the sheet metal has the task of pressing the sheet metal against the support, as well as shaping the internal bending radius. The shaping roller is positioned so that it is under the sheet metal - its task is to shape the sheet metal on its outer surface. Both rollers in the process are driven by induction motors, so they rotate in opposite directions. It is possible to shape without a preset rotational movement. The rollers will rotate as a result of contact between the tool surfaces of and the sheet metal generating frictional forces. Both the shaping roller and the support roller can move in the vertical axis. The shaping roller also has the ability to move in the horizontal axis. It is possible

[1] Department of Metal Forming, Lublin University of Technology, Nadbystrzycka 38D, Lublin, Poland, jaroslaw.wojcik@pollub.pl

to change the distance between the rollers. In addition, the shaping roller can be tilted during the process. Fig. 1b shows the final stage of the process with the shaped product. Once the semi-finished product is attached and the tools are set, the machine's work table moves along a defined trajectory. During this movement, the rollers incrementally shape the sheet metal. Then, after each pass, the shaping roller moves in the vertical axis, and the machine worktable moves again along the defined trajectory. In the final stage of the process, the support roller also moves in the vertical axis, removing the resulting inaccuracies in the shape of the product.

On the basis of numerical simulations, it was determined that due to such kinematics of tool movement, the product is characterized by better quality - there is no unfavorable folding of the sheet surface. Based on the analysis using FEM, the range of technological parameters for which experimental tests will be carried out has been established. This paper focuses on the results of numerical simulations of the incremental forming process of sheet metal with different thicknesses (ranging from 1 to 5 mm) using three different tool variants. In the cases analyzed, both rollers had the same geometries for the variant. However, it can be assumed that the use of geometrically different rollers for a given variant will affect the quality of the shaped products. Therefore, the choice of geometry of shaping tools has a decisive impact on the quality of products.

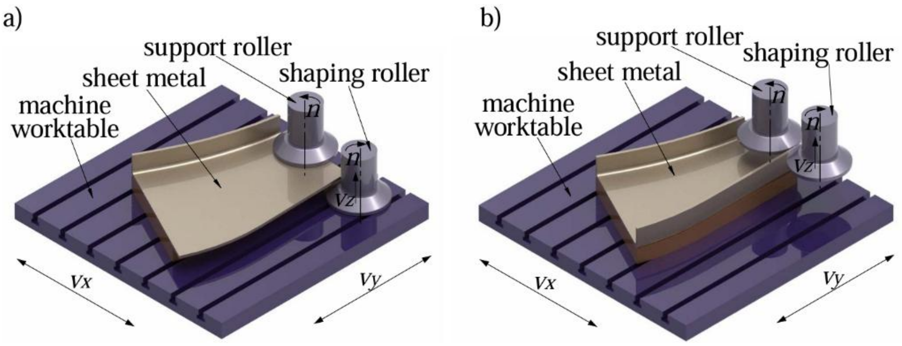

Fig.1. Diagram of incremental sheet metal forming: a) initial stage, b) end of the process

References

[1] *Chang Z., Li M., Chen J., Analytical modeling and experimental validation of the forming force in several typical incremental sheet forming processes, International Journal of Machine Tools and Manufacture, 2019, 140, 62-76.*

[2] *Dang X., He K., Wei S., Li J., Du R., Application of incremental forming in sheet metal bending process, Advanced Materials Research, 2014, 900, 561-564.*

[3] *Gądek T., Majewski M., Nowacki Ł., Drenger T., Tests of forming symmetrical products using the spinning method supported by FEM simulations, Metal Forming, 2019, 30, 273-290.*

Andrzej Gontarz[1], Piotr Surdacki[1], Grzegorz Winiarski[1], Konrad Lis[1]

Selected Aspects of the Rolling Process of Steel Rings Using Sleeves

Abstract

In general, the ring rolling process is divided into two types: radial and radial-axial. For these two types of ring rolling processes, it is difficult to achieve a large increase in ring height. In contrast, in the sleeve ring rolling process, a large increase in both the diameter and height of the ring can be achieved. The proposed forming method mainly ensures the stability and ultimate roundness of the deformed product due to the inner surface of the stop roller, without guide rollers and a complicated control scheme. A schematic of the process is shown in Figure 1.

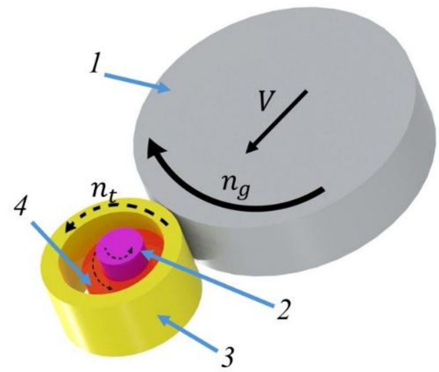

Fig.1 Diagram of the ring rolling process using a sleeve, 1 - main roller, 2 - mandrel, 3 - sleeve, 4 - ring

The entire forming process involves two stages: the radial ring-rolling stage and the axial forming stage (Fig. 2.).

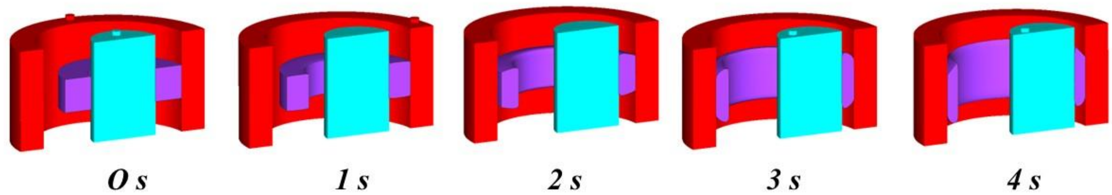

Fig.2. The course of the process

[1] Lublin University of Technology, Faculty of Mechanical Engineering, Nadbystrzycka 36 Str., 20-618 Lublin, Poland, piotr.surdacki@pollub.pl

Numerical analysis of the process was carried out on the basis of the finite element method (FEM), using the software package Simufact Forming 2024.4. The results of the theoretical study are shown in Figure 3.

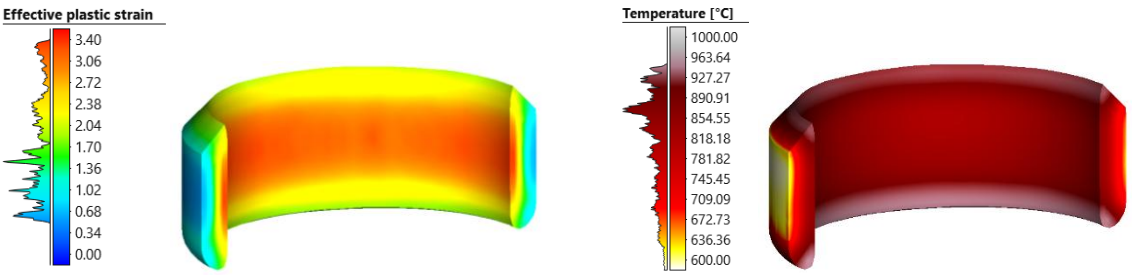

a) b)

Fig.3. Results of numerical analysis, a) effective plastic strain distribution [-], b) temperature distribution [°C]

Based on the results of the analysis, an actual process was carried out, which resulted in a defect-free ring (Figure 4.).

a) b)

Fig.4. Experimental research, a) research site, 1 - main roller, 2 - mandrel, 3 - sleeve, 4 - ring, b) final shaped ring

It should be said that the use of sleeve during the rolling process eliminates defects: ,,fish tail", taper shape, ovalization, polygonal shape. During the process, round rings of a certain outside diameter are obtained, which allows for repeatability of the process and reduction of technological allowances associated with the removal of ovality. The calibration operation is eliminated.

Due to the advantages of controlling the stability and roundness of the ring and achieving a large increase in both the diameter and height of the ring, the proposed ring rolling process has potential.

Piotr Surdacki[1], Andrzej Gontarz[1], Grzegorz Winiarski[1] , Konrad Lis[1]

Analysis of the Influence of Tool Speed on the Cross-Section of the Formed Ring During Ring Rolling in the Sleeve

Abstract

The ring rolling process is generally divided into two types: radial and radial-axial. In both cases, it is difficult to achieve a large increase in ring height and perfectly round rings. In the sleeve ring rolling process, a large increase in both the diameter and height of the ring can be achieved. This molding method ensures the stability and final roundness of the shaped product due to the inner surface of the thrust roller, without guide rollers and a complicated control scheme. A schematic of the process is shown in Figure 1.

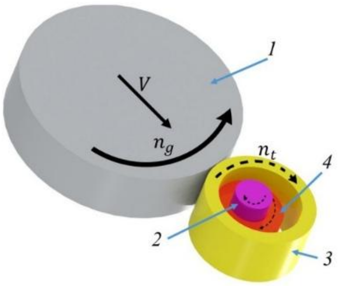

Fig.1. Diagram of the ring rolling process using a sleeve, 1 - main roller, 2 - mandrel, 3 - sleeve, 4 - ring

The article describes the effect of tool speed on the cross-sectional shape of the rings and material loss. Material loss were determined as:

$$\delta = \frac{V_l}{V_0} * 100\% \qquad [1]$$

where:

V_0 – the initial volume of the billet in mm^3,

V_l – the volume of material loss in machining in mm^3, which can be calculated from the following dependence:

$$V_l = V_f - \frac{\pi * \left(D_f^2 - d_f^2\right) * h_{f,min}}{4} \qquad [2]$$

where:

D_f – final outer diameter of the ring,

[1] Lublin University of Technology, Faculty of Mechanical Engineering, Nadbystrzycka 36 Str., 20-618 Lublin, Poland, a.gontarz@pollub.pl

d_f – final inner diameter of the ring,

$h_{f,min}$ – final smallest ring height.

The theoretical analysis of the process was carried out on the basis of the finite element method (FEM), using the software package Simufact Forming 2024.4. The analysis was carried out for a single rotational speed (n_g= 90 RPM), only the infeed speed of the shaping tool was changed (V = 1 mm/s, 3 mm/s, 5 mm/s, 7 mm/s, 9 mm/s). A defective ring was obtained for the higher addition speed. The results of the analysis are shown in Figure 2. The Figure 2 c shows the loss of material for each variant of the analysis. Figure 3 shows the material loss values as a function of feed speed.

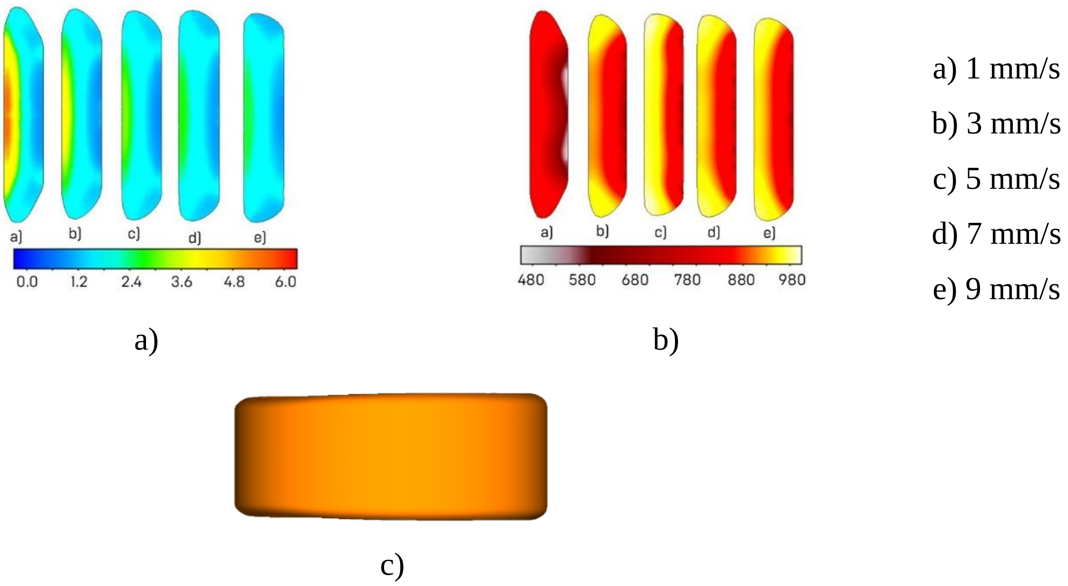

Fig.2. Results of theoretical analysis, a) strain distribution [-], b) temperature distribution [°C], c) defective ring shaped at: V = 10 mm/s, n_g= 90 RPM

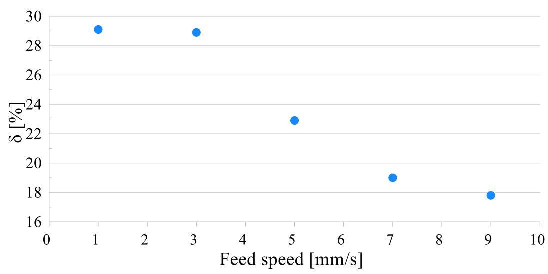

Fig.3. Coefficient δ as a function of feed speed

Due to the advantages of controlling the stability and roundness of the ring and the height of the ring, the cylindrical ring rolling process analyzed has potential and prospects in the production of thin-walled cylindrical rings. However, it is important to properly select the speed parameters.

Kacper Preisnar

Validation of turbocharger compressor cooling using pulsating heat pipes using computational fluid dynamics simulations and bench tests.

Abstract

The aim of the work was to develop and validate an innovative turbocharger compressor cooling system using Pulsating Heat Pipes (PHP) [1]. The main problem that was solved was the phenomenon of oil coking in the cold part of the turbocharger, which negatively affected its efficiency and service life. Traditional cooling methods, such as water jackets, would require interference with the engine cooling system, which was unacceptable for BorgWarner customer. During the work, two numerical models of the turbocharger were prepared - one without cooling, the other with PHP cooling - and CFD (Computational Fluid Dynamics) simulations were carried out using conjugate heat transfer (CHT - Conjugate Heat Transfer). The models took into account the full geometry of the turbocharger, including the compressor and turbine sides, as well as a carefully prepared computational mesh. The cooling model used four PHP loops made of 4 mm copper tubes, arranged in the compressor and bearing housing. The spaces between the tubes and the housing were filled with thermally conductive grease. Simulations showed that the use of PHP allows for a reduction in the air temperature at the compressor outlet by about 7–8°C and a significant reduction in the temperature of solid elements, which can effectively reduce the phenomenon of oil coking. In order to validate the simulation results, bench tests were performed on a prototype turbocharger equipped with PHP. The tests confirmed the effectiveness of cooling – a temperature drop of 8–10°C was observed at key measurement points. Additionally, thanks to the use of a thermal imaging camera, the pulsating nature of the heat pipes' operation was confirmed.

References

[1] *S. Khandekar, P. K. Panigrahi, F. Lefèvre, and J. Bonjour. Local hydrodynamics of flow in a pulsating heat pipe: A review. Frontiers in Heat Pipes, 2010. [2] Eremeyev V.A., Rosi G., Naili S., Surface/interfacial anti-plane waves in solids with surface energy, Mechanics Research Communications 2016, 74, 8-13.*

Feliks Stachowicz[1]

Change of surface topography of copper sheets as a result of plastic deformation

Abstract

It is common knowledge that the plastic properties of metallic materials depend on their internal structure. For many materials, this relationship can be described by the Hall-Petch equation, which indicates (among other things) a linear relationship between the yield stress and the inverse square root of the grain size - $\sigma = \sigma^0 + k^\sigma d^{-0.5}$, where: σ^0 - initial yield stress, d – average grain size.

The grain size in plastically deformed sheets also affects the intensity of changes in the surface topography, which results, among others, from changes in the material structure - reorientation and deformation of grains (Fig. 1). According to the proposal of Fukuda et al. [2], the intensity of surface roughness increase due to plastic deformation depends on the grain size: $R = R^0 + k^R d\varepsilon_e$. The results of our own research [3] have shown that more accurate description of this relationship can be obtained by introducing the square root of the grain size into this equation: $R = R^0 + k^R d^{0.5}\varepsilon_e$.

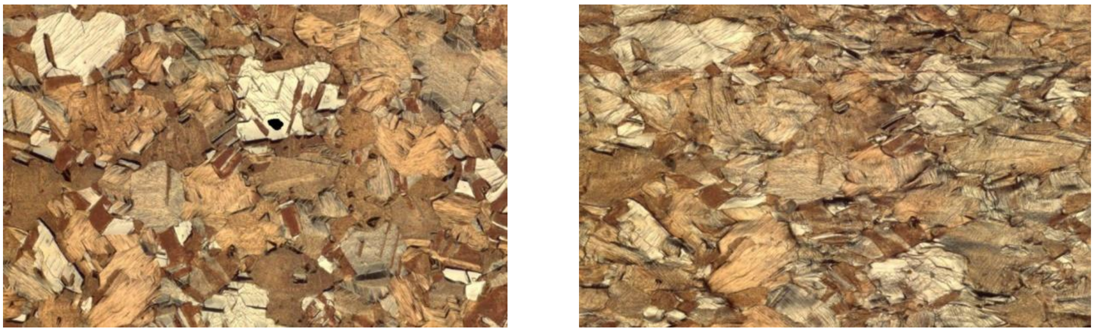

Fig.1 Microstructure of the samples before deformation (left) and after deformation to the value of ε=0.35 (right)

The results of experimental measurements of the surface roughness parameter Rmax of copper sheets with different grain sizes plastically deformed in uniaxial and biaxial tensile tests (hydraulic bulging) allowed the determination of the following relationships - Table 1.

[1] Katedra Przeróbki Plastycznej, Politechnika Rzeszowska, Al. Powst. Warszawy 8, stafel@prz.edu.pl

The aim of this study is to propose that a linear equation indicating a linear relationship between the value of the "surface smoothness" parameters and the inverse square root of the grain size should be used to describe changes in the surface topography of plastically deformed copper and brass sheets, similarly to the Hall-Petch equation - $S = S^0 + k^S d^{0.5}$εe. The surface smoothness parameters are defined as the inverse of the roughness parameters Smax = 1/Rmax.

Table.1 The value of the surface roughness parameter Rmax as a function of effective strain of copper sheets with different grain sizes

Grain size µm	**Square root of grain size, µm$^{-0.5}$**	**Equations describing the dependence of the Rmax parameter on the effective strain**
48.8	6.98	Rmax = 3.2 +31.3 ε_e
79.9	8.93	Rmax = 2.9 +40.4 ε_e
110.7	10.52	Rmax = 3.0 +45.9 ε_e
134.1	11.58	Rmax = 3.2 +70.2 ε_e

The analysis of the obtained results showed a linear relationship between the changes in the surface topography of copper sheets with different grain sizes as a result of plastic deformation (Fig. 2) - the lowest agreement in the description of this relationship was found using the equation according to Fukuda et al. [2], and the best when introducing the proposed "surface smoothness" parameter.

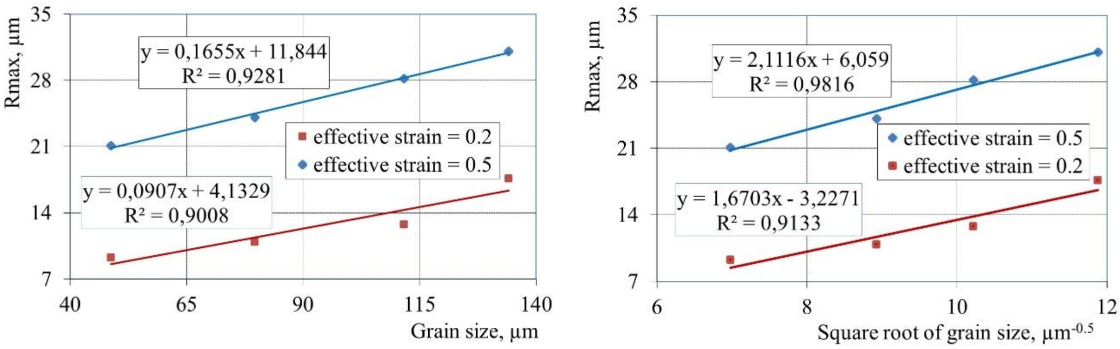

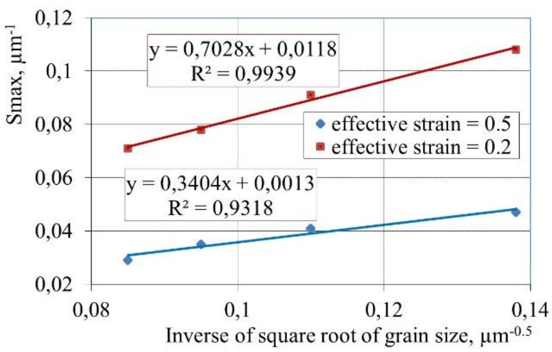

Fig.2 Comparison of the accuracy of the description of the dependence of the surface topography parameter value on the grain size of deformed copper sheets using the equations: according to [2] - upper left graph; according to [3] - upper right graph; and according to the new proposal - lower graph

References

[1] Meakin J.D., Petch N.J.: Strain hardening of polycrystals: the α-brasses, Philosophy Magazine, 1974, 29, 1149-1156.

[2] Fukuda, M., Yamaguchi, K., Takakura, N., Sakano, Y.: Roughening phenomenon on free surface of products in sheet metal forming, Journal of the JSTP, 1974, 15, 994-1002.

[3] Stachowicz F.: On the connection between microstructure and surface roughness of brass sheets and their formability, Acta Mechanica, 2016, 227, 253-262.

Tomasz Kusiak[1], Janusz Tomczak[1], Jarosław Wójcik[1]

Effect of normalizing annealing on the microstructure and mechanical properties of bimetals produced in a CNC skew rolling mill

Abstract

Contemporary technological development generates a growing demand for new engineering materials, such as bimetals, which combine different metal properties within a single structure. One of the modern methods for their production is skew rolling, performed using an innovative three-roll CNC skew rolling mill. This technology enables the durable bonding of two metals or alloys with differing properties, while simultaneously allowing for the formation of axisymmetric products or semi-finished products with variable cross-sections, without the need for costly, dedicated tooling [1, 2]. Thanks to lower rolling forces compared to conventional methods, it is also possible to significantly reduce energy consumption and production costs, which is particularly important in low-volume or unit production [3].

The aim of this study was to determine the effect of normalizing annealing on the quality of the bond in a C60/S355 bimetallic rod produced using skew rolling technology (Fig. 1).

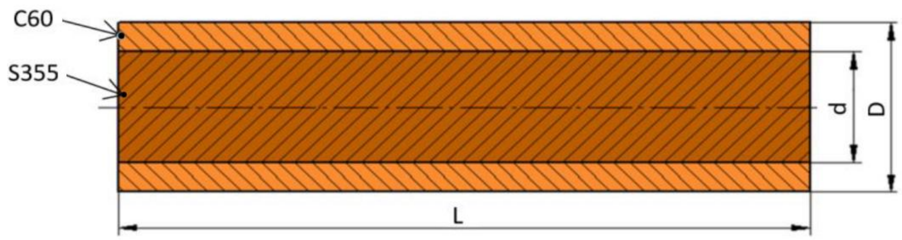

Fig. 1. Schematic of the C60/S355 bimetallic rod; L – length, D – diameter of the outer layer, d – diameter of the core

Normalizing annealing is a heat treatment process involving heating the material to an appropriate temperature, followed by controlled cooling, in order to obtain a homogeneous microstructure and improve mechanical properties. This process enables the structural alignment of the bimetal layers and increases the strength of their bond, which is crucial for structural components requiring a combination of diverse material properties.

Two technological variants were examined, differing in the heating atmosphere of the billet to a temperature of 1180 °C – one without protection and the other in a protective

[1] *Department of Metal Forming, Faculty of Mechanical Engineering, Lublin University of Technology, Nadbystrzycka 38 D, 20 – 618 Lublin, Poland*

atmosphere to prevent decarburization of the bonding surface. The analysis covered microstructure, average grain size, microhardness, and shear strength after the normalizing process.

The results showed that normalizing annealing positively influences the improvement of microhardness and the durability of the bimetal, enhancing its functionality in further engineering applications.

References

[1] *Tomczak, J.; Bulzak, T.; Pater, Z.; Wójcik, Ł.; Kusiak, T. Skew rolling of bimetallic rods. Materials 2021, 14, 18.*

[2] *Tomczak, J.; Pater, Z.; Bulzak, T.; Lis, K.; Kusiak, T.; Sumorek, A.; Buczaj, M. Design and technological capabilities of a CNC skew rolling mill. Arch. Civ. Mech. Eng. 2021, 21, 72*

[3] *Pater Z.; Tomczak J.; Lis K.; Bulzak T.; Shu X. Forming of rail car axles in a CNC skew rolling mill. Arch. Civ. Mech. Eng. 2020, 20, 69.*

Emil Spišák[1], Janka Majerníková[1], Peter Mulidrán[1]

Optimization of technological parameters when drawing cups from steel sheets

Abstract

The article deals with the evaluation of the deep drawing process of steel sheets, particularly the height of the yield edges because of the anisotropic behavior of these materials. Two high-strength steel sheets - microalloyed steel HX420 with a thickness of 0.7 mm and steel with transformation-induced plasticity TRIP RAK40/70 with a thickness of 0.75 mm - were the subject of the investigation. The plastic behavior of the material was experimentally verified by drawing cups from circular blanks with a size of 63 mm using a cupping test. The prediction of the output parameters consisted in the use of strengthening models according to Hollomon and Krupkowski, together with plasticity theories according to Hill48 and Barlat, using implicit and explicit simulation.

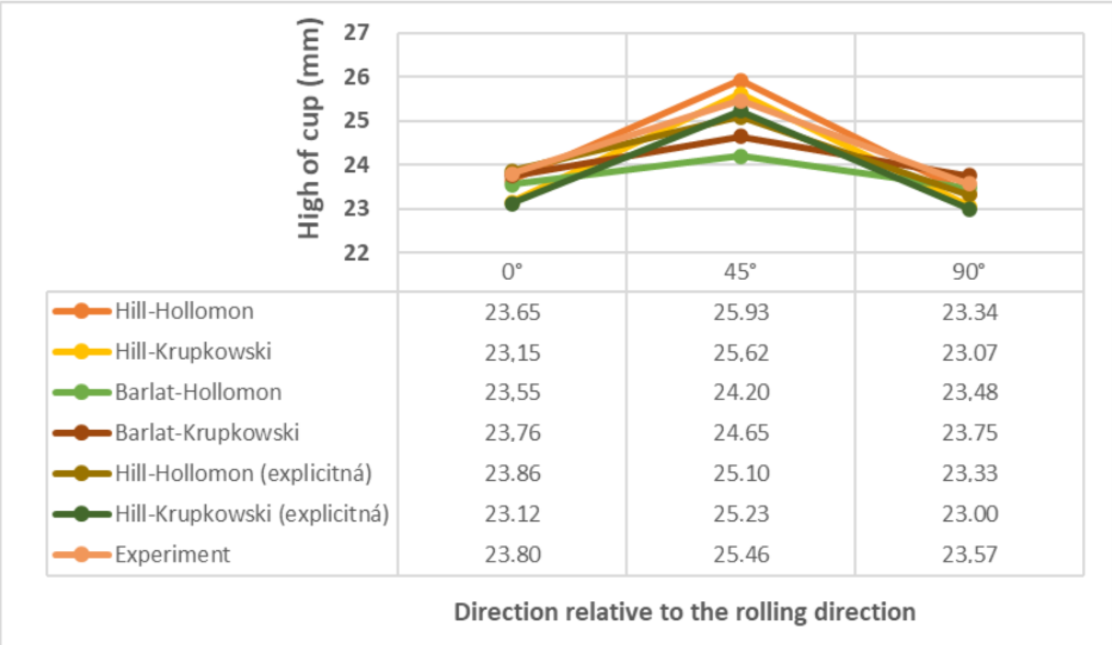

	0°	45°	90°
Hill-Hollomon	23.65	25.93	23.34
Hill-Krupkowski	23,15	25.62	23.07
Barlat-Hollomon	23,55	24.20	23.48
Barlat-Krupkowski	23.76	24.65	23.75
Hill-Hollomon (explicitná)	23.86	25.10	23.33
Hill-Krupkowski (explicitná)	23.12	25.23	23.00
Experiment	23.80	25.46	23.57

Fig.1 Comparison of the ear height for material HX420

[1] Faculty of Mechanical Engineering, Technical University of Košice, Mäsiarska 74, Košice, Slovakia, emil.spisak@tuke.sk, janka.majernikova@tuke.sk, peter.mulidran@tuke.sk

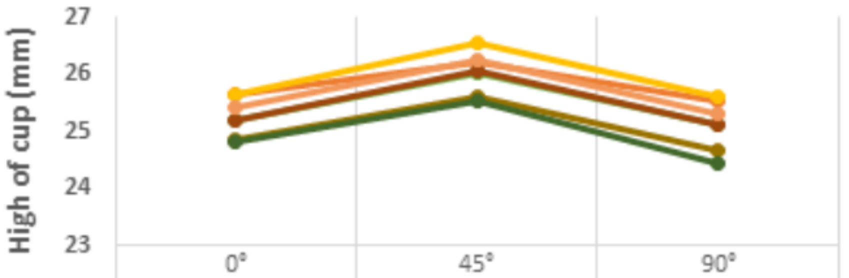

	0°	45°	90°
Hill-Hollomon	25.63	26.23	25.55
Hill-Krupkowski	25.66	26.55	25.60
Barlat-Hollomon	25.2	26.03	25.11
Barlat-Krupkowski	25.19	26.06	25.12
Hill-Hollomon (explicitná)	24.87	25.61	24.66
Hill-Krupkowski (explicitná)	24.8	25.52	24.43
Experiment	25.41	26.26	25.31

Direction relative to the rolling direction

Fig.2 Comparison of the ear height for material TRIP

Conclusion

Based on the results obtained from the simulations, we can conclude that for material HX420 (Fig. 1) the models using the theory according to Hill appeared to be the most ideal. In the case of the TRIP RAK40/70 material (Fig. 2) the cups have relatively little earrings. The deviations of the individual models are not large.

Acknowledgement

This research was funded by the Slovak Research and Development Agency under project APVV-21-0418 and by the projects KEGA 018TUKE-4/2024.

References

[1] Mulidrán, P.; Spišák, E.; Tomáš, M.; Majerníková, J.; Rohaľ, V. Numerical simulation of bending steels used in automotive industry with emphasis on springback. Acta Metallurgica Slovaca 2024, 30, 41-46.

[2] Mulidrán, P.; Spišák, E.; Tomáš, M.; Majerníková, J.; Varga, J. The effect of material models in the FEM simulation on the Springback prediction of the TRIP steel, Acta Metallurgica Slovaca 2021, 27, 103-108.

[3] Mulidrán, P.; Spišák, E.; Tomáš, M.; Majerníková, J.; Bidulská, J.; Bidulský, R. Impact of Blank Holding Force and Friction on Springback and Its Prediction of a Hat-Shaped Part Made of Dual-Phase Steel, Materials 2023, 16, 811.

[4] Spišák, E.; Majerníková, J.; Mulidrán, P.; Hajduk, J.; Ruda, F. Springback Analysis and Prediction of Automotive Steel Sheets Used in Compression Bending, Materials, 2025, 18, 1-15.

Grzegorz Winiarski[1], Andrzej Skrzat[2], Marta Wójcik[3]

Analysis of selected fracture criteria in the radial extrusion process

Abstract

Radial extrusion of hollow products is a method in which the direction of flow of the material is perpendicular to the direction of movement of the punch. As a result, it makes it possible to shape products that have lateral projections in the form of flanges and steps, among others. One of the limitations of the technology is the possibility of material cracking, which affects the achievable maximum diameter of the extruded flange [1, 2]. The realized research focuses on the analysis of the process with special attention to the phenomenon of cracking. Their goal is to determine the possibility of predicting the loss of material cohesion at the stage of technology design. As part of the research, an advanced numerical model of the radial extrusion process was developed, which will allow a detailed analysis of the process flow and kinematics of the deformed material.

A radial extrusion process was analyzed using a hollow billet with dimensions ø20 x ø14 x 80 mm made of EN AW 6060 aluminum alloy. It was assumed that the process would be carried out under cold forming conditions, and the initial temperature of the billet and tools was assumed to be 20°C. The height of the die zone in which the extruded flange is shaped was assumed to be equal to the wall thickness of the billet, i.e. 3mm. Studies on the phenomenon of cohesion loss of the material were realized based on numerical calculations. In these, four different fracture criteria were adopted, i.e. Cockcroft and Latham, Ayada, Brozzo and Oh.

The distributions of the values of each damage function at the moment when the flange reaches its maximum diameter (due to cracking) are shown in Figure 1. It can be seen that for each criterion the maximum values are located at the flange edge. This is in agreement with the results of experimental studies, which indicate that cracking occurs in the aforementioned zone [3].

[1] Department of Metal Forming, Faculty of Mechanical Engineering, Lublin University of Technology, ul. Nadbystrzycka 36, 20-618 Lublin, Poland, g.winiarski@pollub.pl
[2] Department of Materials Forming and Processing, Faculty of Mechanical Engineering and Aeronautics, Rzeszow University of Technology, Al. Powstańców Warszawy 8, 35-959 Rzeszów, Poland, askrzat@prz.edu.pl
[3] Department of Materials Forming and Processing, Faculty of Mechanical Engineering and Aeronautics, Rzeszow University of Technology, Al. Powstańców Warszawy 8, 35-959 Rzeszów, Poland, m.wojcik@prz.edu.pl

The conducted research made it possible to determine the limits values of each fracture criterion, which makes it possible to predict the moment and location of material cohesion loss on the basis of numerical calculations.

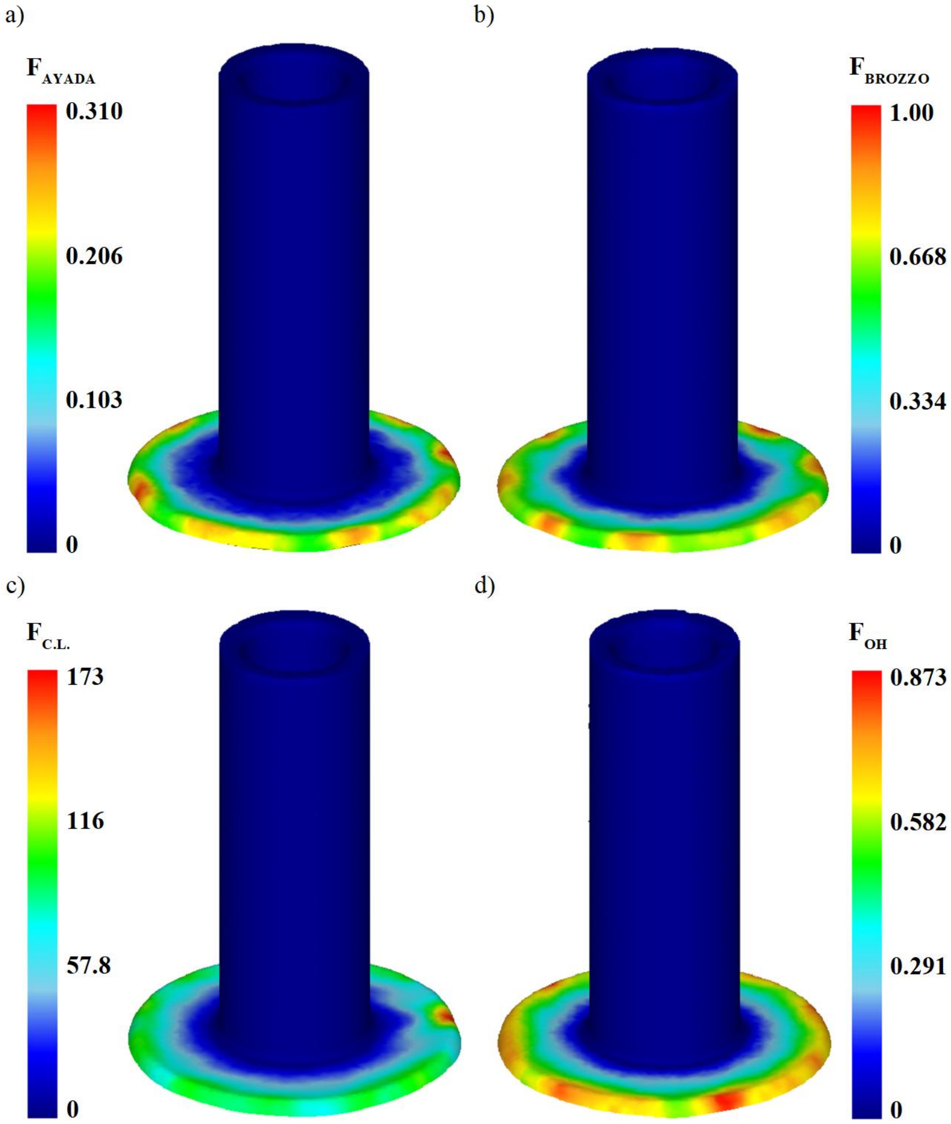

Fig.1. Distribution of damage function according to: a) Ayada, b) Brozzo, c) Cockcroft and Latham (in MPa), d) Oh in flanged hollow product

References

[1] Winiarski G., New method for detecting flange fracture initiation in incremental radial extrusion, Materials 2024, vol. 17, nr 5, pp. 1-14.

[2] Winiarski G., Gontarz A., Samołyk G., Flange formation in aluminium alloy EN AW 6060 tubes by radial extrusion with the use of a limit ring, Archives of Civil and Mechanical Engineering 2019, vol. 19, nr 4, pp. 1020-1028.

[3] Winiarski G., Samołyk G., New methodology for predicting the cracking phenomenon in the radial extrusion process of hollow parts with a flange, Advances in Science and Technology Research Journal, 2023, vol. 17, nr 3, pp. 64-72.

Jacek Michalczyk

Modelling of manufacturing processes for cylindrical products witch splines

Abstract

Splines are used to create spline, or movement, connections without any intermediate components. They are usually used to fit hubs onto shafts. Splines are more difficult to manufacture than keyed shafts, but are more durable, longer-lasting and therefore used in more responsible applications. Spline (multi-spline) shafts allow high torsional moments to be transmitted. As standard, for normal conditions, they are manufactured using CNC technology from C45 steel (to ESN 12 050), according to ISO14 (DIN 5463). Components with splines are manufactured using conventional CNC technology. As is well known, CNC technology ensures high dimensional accuracy, so it is not possible to eliminate it completely from the manufacturing process. The disadvantage of CNC is the low material yield due to the large waste material created during the cutting process, especially when the feedstock for a spline cylinder is a rod or disc reaching up to 45% of the total material volume. In order to increase the yield of the material, plastic forming was proposed by using two methods of shaping by extrusion and pressing. The forming methods are proprietary developments that are patents for inventions. Process modelling was carried out using materials typical of this type of product, i.e. C45 steel and Rg 7 bronze.

Extrusion methods

1 Extrusion and flange pressing.

The method consists of placing a cylindrical charge in a tubular container on a pressing mandrel. The mandrel has a chamfered top edge at an angle of approximately 30° to the vertical axis. The workpiece is pressed with the top punch causing radial and angular concurrent extrusion. The feedstock is extruded through the opening of the annular die, between the eyelet of the annular die and the pressing mandrel, forming a conical sleeve with an internal diameter larger than the diameter of the pressing mandrel. The feedstock is pressed with the top punch until a conical sleeve with a bottom thickness determined before the process starts is extruded through the opening of the annular die. Subsequently, the annular die, which has a slanted, two-stage inner wall with the slope of the wall on the tubular side corresponding to the chamfer angle of the top edge of the pressing mandrel, is moved downwards along the pressing mandrel. Thus, further plastic shaping of the tapered sleeve is carried out by lengthening and reducing its wall thickness. As a result of the pressure of the annular die on the wall of the conical bushing, its resulting flange is initially rolled out at the junction of the mandrel and its flange base. A schematic diagram of the process is shown in Fig.1.

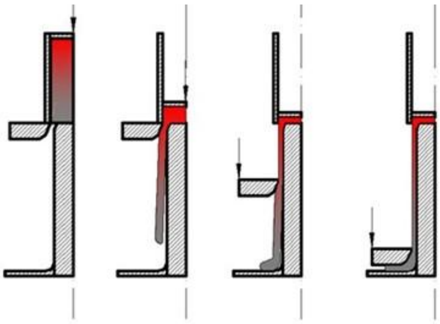

Fig.1 Method of extruding and pressing the sleeves

2. Variable section extrusion

The method is an adaptation of the extrusion of cylinders with a variable cross-section spigot. The punch, by applying pressure to the feedstock in the form of a rod, deforms it in such a way that, entering the sleeve in strips, it gradually pushes the feedstock out of the sleeve, causing it to swell outside the sleeve area. Once the charge is completely removed from the sleeve, the locking mechanism is released and the sleeve is pushed down the cylindrical container by the flanged end of the punch. At the same time, together with the punch, the previously swollen charge is extruded through the clearance between the cylindrical container and the tool plate. Once the feedstock has been extruded through the punch and sleeve, a complex-shaped sleeve is obtained, followed by the partial removal of the ejector from the tool plate and the belted entry of the punch into its opening, which makes a hole in the product spigot. A schematic diagram is shown in Figure 2.

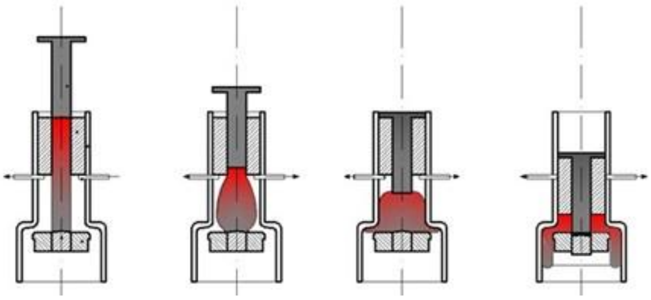

Fig.2 Schematic diagram of the extrusion of a variable cross-section sleeve

References

[1] Michalczyk J., Wencel S.: Tool for producing flanged sleeves. Polish Patent Pat.235009.

[2] Michalczyk J., Mróz S., Wencel S. Szota P.: Method of manufacturing cylindrical products with a spigot of variable longitudinal section. Polish Patent Pat.236910.

Janette Brezinová[1]

Possibilities of using manual laser welding in joining aluminum alloys

Abstract

The paper presents the results of research aimed at determining the quality of welds using manual laser welding. The influence of welding parameters on the quality of welds was evaluated. Two types of filler materials were used - AlSi5 and AlMg3. The basic material was an aluminum alloy of the Roll bonding type. Roll bonding (RB) describes solid-state manufacturing processes where cold or hot rolling of plates or sheet metal is carried out for joining similar and dissimilar materials through the principle of severe plastic deformation. The quality of welds was evaluated by visual examination, determination of weld microhardness and static tensile test.

[1] Faculty of Mechanical Engineering, Technical University of Kosice, Mäsiarska 74, Kosice, Slovakia,

Łukasz Wójcik[1]

Physical Modelling with Plasticine for Phenomena Identification in Cross-Wedge Rolling

Abstract

The conducted research focuses on the physical modelling of the cross-wedge rolling process, utilizing commercial PRIMO plasticine as a material to simulate hot-formed steel. Physical modelling is a recognized simulation method that facilitates the analysis of processes and phenomena occurring during plastic metal forming. The main advantages of this method include the ability to conduct experiments and preliminary studies in laboratory conditions, without the need to involve an industrial environment. This significantly reduces costs and allows for real-time observation of the forming process. n this part of the research, physical modelling of the Mannesmann phenomenon was performed using the channel-pressing method. The obtained results were compared with data for C45, 50HS, and R260 steels. The final phase of the research focused on the possibilities of physically modelling limitations encountered during cross-wedge rolling, such as internal cracks, slips, necking, and ruptures of the formed product.

Internal cracks, known as the Mannesmann effect, are characterized by the formation of porosities and cracks within the formed product. Model studies of the Mannesmann phenomenon were conducted using the rotary disk pressing method in a channel. Samples with dimensions of Ø40×20 mm were heated in an electric chamber furnace to temperatures of 950°C, 1000°C, 1050°C, 1100°C, and 1150°C. These studies allowed for precise determination of the path along which the sample fractured.

In the case of model studies, white and black PRIMO plasticine was used, and the processes were carried out at scales of 1:2 or 1:2.5 relative to actual tools. Model studies were conducted for six temperatures: 0°C, 5°C, 10°C, 12°C, 15°C, and 20°C. The possibility of using commercial PRIMO plasticine (white and black) as modeling materials for physical studies of the Mannesmann phenomenon by the channel-pressing method was confirmed.

The final phase of the research focused on the possibilities of physically modelling various limitations occurring during cross-wedge rolling, including internal cracks, slips,

[1] Lublin University of Technology, Department of Metal Forming, Nadbystrzycka 38D, 20-618 Lublin, Poland

necking, and ruptures of the formed product. These phenomena are often caused by improper selection of the geometric parameters of the forming tools, such as the forming angle (α) and the wedge opening angle (β). The recommended forming angle ranges from 15° to 40°. Increasing this angle value leads to an increase in the tensile force on the forging, which can result in the formation of necking on the material surface. Conversely, an excessively small angle (below 15°) promotes the formation and propagation of cracks within the product. The wedge opening angle should be selected from the range of 3° to 15°. Decreasing this angle shortens the tools, while exceeding 15° can lead to uncontrolled slips between the material and the tools.

Actual experiments were conducted on C45 steel formed at a temperature of 1150°C. Three different sample diameters were used: Ø26×210 mm, Ø33×150 mm, and Ø40×210 mm. The tools for internal crack studies had a forming angle α=−15° and a wedge opening angle β=−10°, which was intended to initiate crack formation along the product's axis. The tools for studying slips, necking, and ruptures were characterized by a forming angle α=45° and a wedge opening angle β=11°. The studies revealed the presence of axial cracks of various diameters and lengths in the samples. Screw-type necking was observed on samples with medium and largest diameters, which initiated rupture.

Model studies were conducted using white and black commercial PRIMO plasticine, applying a 1:2.5 scale relative to the actual tools. The forming temperature of the modelling materials was set at 5°C, which corresponded to C45 steel formed at 1050°C. Model samples had dimensions of Ø10.4×84 mm, Ø13.2×60 mm, and Ø16×40 mm, allowing for three different degrees of reduction. It was found that material cracking within the forging could not be modelled, but the physical modelling of other limitations (slips, necking, ruptures) was successfully carried out.

The conducted theoretical and experimental studies confirmed that physical modelling with commercial plasticine allows for the analysis of material flow kinematics and the prediction of force parameters and occurring limitations. Finally, the physical modelling of cross-wedge rolling showed high convergence of results with actual studies, both in terms of force parameters, shape, and product defects.

Konrad Lis[1], *Piotr Surdacki*[2]

Analysis of the Effect of Skew Rolling Parameters on the Radial Force Using Machine Learning Methods

Abstract

This paper presents the application of machine learning regression models for the prediction of radial force acting on a tapered roll during the skew rolling process. The aim of the study is to develop data-driven models that allow for accurate estimation of process forces without the need for time-consuming and computationally intensive FEM simulations [1]. This approach facilitates the faster development of rolling parameters and tool geometries, significantly shortening the preparatory phase of manufacturing. Machine learning methods are already being used in sheet metal forming in particular to detect material defects [2, 3].

The study was based on experimental data obtained during skew rolling of stepped shafts made of C60-grade steel [4]. Three models were evaluated: Support Vector Regression (SVR), Random Forest Regressor, and XGBoost Regressor (XGB). The input parameters included the forming angle α, skew angle θ, reduction ratio δ, and axial chuck velocity V_u. The radial force values were used as the prediction target. Evaluation metrics included the coefficient of determination (R^2) and root mean square error (RMSE) for both training and test datasets.

The results indicate that all models achieved a satisfactory level of generalization. The Random Forest Regressor provided the best performance on the training set ($R^2 = 0.86$, RMSE = 3.12 kN) and also maintained strong generalization to the test set ($R^2 = 0.83$, RMSE = 2.92 kN). The SVR model, however, showed the higher training accuracy ($R^2 = 0.88$, RMSE = 2.9 kN) and maintained very good performance on the test set ($R^2 = 0.85$, RMSE = 2.73 kN), indicating strong generalization and minimal overfitting. XGBoost achieved the highest R^2 (0.94) and lowest RMSE (2.15 kN) on the training set, although with slight performance degradation on the test set ($R^2 = 0.85$, RMSE = 2.74 kN), suggesting some degree of overfitting.

The use of machine learning models to predict radial forces opens a promising alternative to finite element simulations in skew rolling. These models can significantly enhance process

[1] Faculty of Mechanical Engineering, Lublin University of Technology, Nadbystrzycka 38D Str., Lublin, Poland, k.lis@pollub.pl
[2] Faculty of Mechanical Engineering, Lublin University of Technology, Nadbystrzycka 38D Str., Lublin, Poland, k.lis@pollub.pl

design efficiency by enabling rapid force estimations during parameter tuning. In the next stage of research, the models will be extended to predict radial forces for various stepped roll geometries, further supporting flexible and automated rolling setups.

References

[1] Pater Z., FEM analysis of loads and torque in a skew rolling process for producing axisymmetric parts, Archives of Metallurgy and Materials, 2017, 62, 85–90.

[2] Lechwar S., Pietrzyk M., Rauch Ł., Problem klasyfikacji wad typu zgorzelina występujących w walcowni gorącej blachy, Mechanik, 2013, 86, 880–886. (In Polish)

[3] Kurra S., Rahman N.H., Regalla S.P., Gupta A.K., Modeling and optimization of surface roughness in single point incremental forming process, Journal of Materials Research and Technology, 2015, 4, 304–313.

[4] Lis K., Analysis of the Effect of Skew Rolling Parameters on the Surface Roughness of C60 Steel Products Using ML Methods, Materials, 2023, 16, 7136.

Wiesław Frącz[1], Iwona Zarzyka[2], Grzegorz Janowski[1], Łukasz Bąk[1]*

SELECTED PROCESSING PROBLEMS OF CHOSEN COMPOSITIONS PHA - BASED POLYMERS WITH POLYURETHANES MODIFIERS

Abstract

The paper presents the problems of processing modern polymer compositions of chosen compositions PHA - based polymers with polyurethanes modifiers.

In particulary the effect of polyurethane addition in amounts of 5, 10 and 15% on the processing properties of compositions produced from P3HB and PHBV was investigated. Modifications of P3HB and PHBV with polyurethanes improve the properties of the compositions in selected areas of application. The method of manufacturing the compositions by extrusion and the injection molding process of specimens for testing the mechanical properties of the produced material are presented. The range of processing parameters used in manufacturing was indicated and the properties of the obtained composition were characterized. The test specimens were produced by means Dr Boy 55E injection molding machine. The parameters of the injection molding process were determined based on experience with similar materials and with the help of the Priamus® system. Particular attention was paid to technological problems occurring in given configurations of processing parameters for both technologies. Methods, the influence of some external factors and some technical solutions that allow processing technologies to be carried out in a satisfactory manner are indicated. Processing temperature, the residence time of the material in the plasticizing system of machines, methods of cooling products and their defects depending on the method of used technological process were considered, especially. Selected processing parameters are presented in Tables 1-3.

Table.1 Processing parameters of the PHBV + 10% PUR composition on a ZAMAK RES-2P12A Explorer twin-screw extruder

Head	Zone 7	Zone 6	Zone 5	Zone 4	Zone 3	Zone 2	Zone 1	Charge
160°C	160°C	160°C	160°C	160°C	160°C	155°C	145°C	50°C

1 Powstancow Warszawy 8 (Rzeszow University of Technology, Dept of Materials Forming and Processing Rzeszow, Poland)
2 Powstancow Warszawy 6 (Rzeszow University of Technology, Dept of Organic Chemistry, Poland).
*Corresponding author: wf@prz.edu.pl:, Tel.:+48178651714, Powstancow Warszawy 8, 35-959 Rzeszow, Poland

Table.2 Processing parameters of the P3HB + 10% PUR composition on a ZAMAK RES-2P12A Explorer twin-screw extruder

Head	Zone 7	Zone 6	Zone 5	Zone 4	Zone 3	Zone 2	Zone 1	Charge
173ºC	173ºC	173ºC	172ºC	172ºC	171ºC	171ºC	170ºC	50ºC

Table.3 The injection parameters of specimens from PHBV composition with 10% polyurethane

Parameter	Value
Mold temperature [°C]	60
Melt temperature [°C]	167
Cooling time [s]	25
Packing time [s]	25
Packing pressure [MPa]	30
Flow rate [cm^3/s]	35

Acknowledgement

The research was carried out as part of the cooperation of inter-university research teams from the VIA CARPATIA 2023 Polytechnic Network - ISKRA project: Research on the impact of modifications of biodegradable aliphatic polyesters on the processing and functional properties of innovative polymer compositions.

References

[1] Białkowska A., Krzykowska B., Zarzyka I., Bakar M., Sedlarik V., Kovarova M., Czerniecka-Kubicka A., Polymer/layered clay/polyurethane nanocomposites: P3HB hybride nanobiocomposites – preparation and properties evaluation, Nanomaterials, 2023, 13, 225.

[2] Eesaee M., Ghassemi P., Nguyen D.D., Thomas S., Elkoun S., Nguyen-Tri P., Morphology and crystallization behaviour of polyhydroxyalkanoates-based blends and composites: A review, Biochemical Engineering Journal, 2022, 187, 108588.

[3] Fernández-Ronco M.P., Gradzik B., Gooneie A., Hufenus R., El Fray M., Tuning poly(3-hydroxybutyrate) (P3HB) properties by tailored segmented biocopolymers, ACS Sustainable Chemistry & Engineering, 2017, 5, 11060–11068.

[4] Frącz W., Janowski G., Bąk Ł., Trzepieciński T., The effect of the extrusion method on processing and selected properties of poly(3-hydroxybutyric-co-3-hydroxyvaleric acid)-based biocomposites with flax and hemp fibers, Polymers, 2022, 14(24), 5370.

[5] Jin P., Pang A., Yang R., Guo X., He J., Zhai J., Study on mechanical properties of polyurethane cross-linked P(E-co-T)/PEG blended polyether elastomer, Polymers, 2022, 14(24), 5419.

[6] Szyszkowska A., Czerniecka-Kubicka A., Pyda M., Byczyński Ł., Gancarczyk K., Sedlarik V., Zarzyka I., Linear polyurethanes with imidazoquinazoline rings – preparation and properties evaluation, Polymer Bulletin, 2019, 76(12), 6343–6370.